



Calhoun: The NPS Institutional Archive
DSpace Repository

Theses and Dissertations

1. Thesis and Dissertation Collection, all items

1958

An investigation of lead zirconate titante.

Rawlins, Robert D.

Monterey, California: U.S. Naval Postgraduate School

<http://hdl.handle.net/10945/14335>

Downloaded from NPS Archive: Calhoun



<http://www.nps.edu/library>

Calhoun is the Naval Postgraduate School's public access digital repository for research materials and institutional publications created by the NPS community. Calhoun is named for Professor of Mathematics Guy K. Calhoun, NPS's first appointed -- and published -- scholarly author.

Dudley Knox Library / Naval Postgraduate School
411 Dyer Road / 1 University Circle
Monterey, California USA 93943

NPS ARCHIVE
1958
RAWLINS, R.

AN INVESTIGATION OF
LEAD ZIRCONATE TITANATE

ROBERT D. RAWLINS

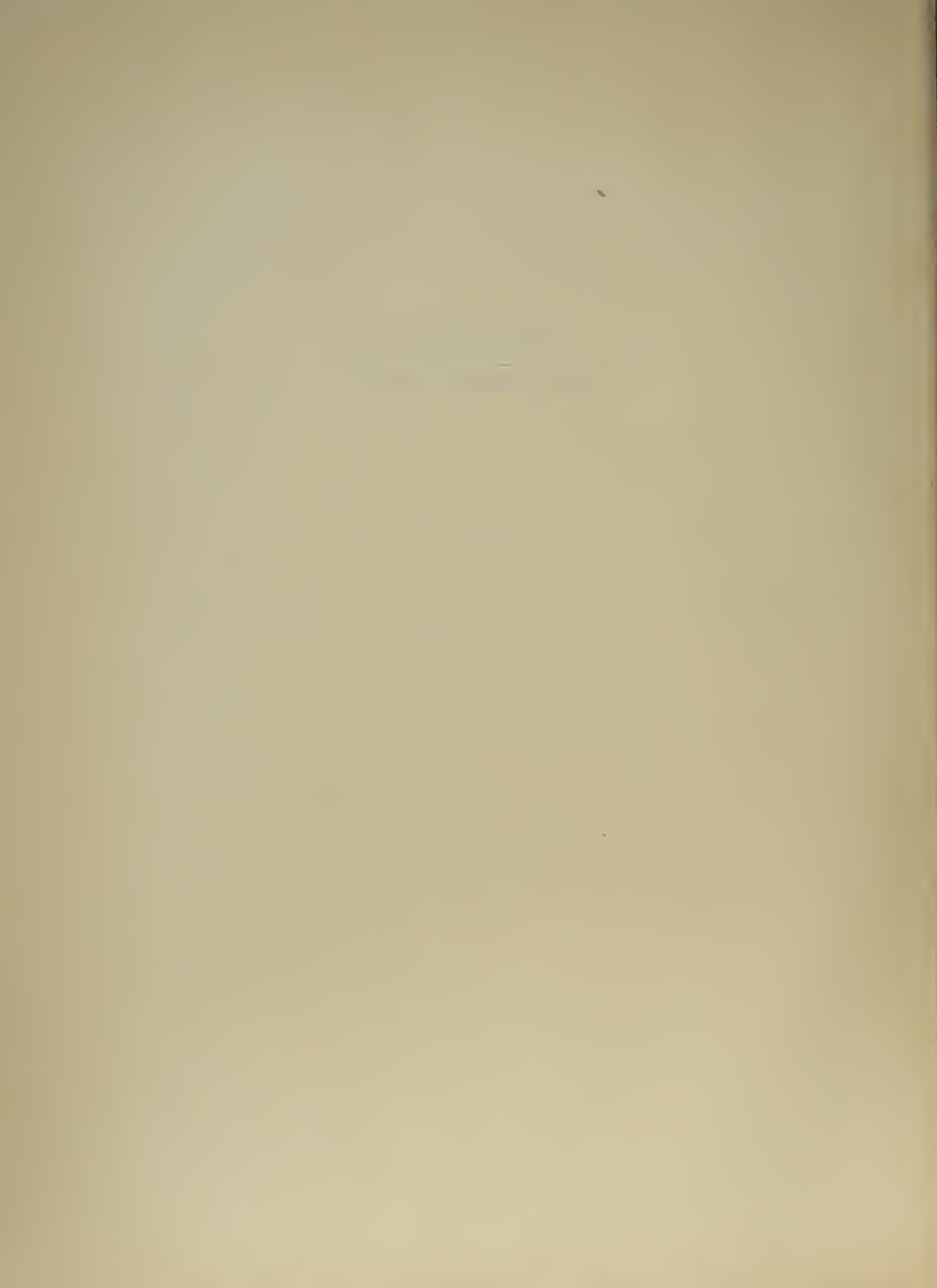
DUDLEY KNOX LIBRARY
NAVAL POSTGRADUATE SCHOOL
MONTEREY CA 93943-5101

AN INVESTIGATION OF
LEAD ZIRCONATE TITANATE

* * * * *

88

Robert D. Rawlins



AN INVESTIGATION OF
LEAD ZIRCONATE TITANATE

by

Robert D. Rawlins
Lieutenant, United States Navy

Submitted in partial fulfillment of
the requirements for the degree of

MASTER OF SCIENCE
IN
ENGINEERING ELECTRONICS

United State Naval Postgraduate School
Monterey, California

1 9 5 8

NPS ARCHIVE

1958

RAWLINS, R.

~~TRAIL~~
~~F2495~~

AN INVESTIGATION OF
LEAD ZIRCONATE TITANATE

by

Robert D. Rawlins

This work is accepted as fulfilling
the thesis requirements for the degree of

MASTER OF SCIENCE

IN

ENGINEERING ELECTRONICS

from the

United States Naval Postgraduate School

ABSTRACT

Although barium titanate has been widely used in acoustic transducers and hydrophones, it has severe shortcomings in high temperature and high power applications. Lead zirconate titanate is a recently developed ferroelectric material which appears to have promise as a transducer material. The piezoelectric and dielectric properties of several lead zirconate compositions are measured over a wide range of temperatures and compared with those properties of a currently used barium titanate ceramic. The dielectric losses of several lead zirconate compositions are investigated under conditions of large driving voltage and high temperature. Finally, the effectiveness of cold versus hot polarization is investigated for a particular lead zirconate composition and a polarizing procedure is described which will produce excellent results.

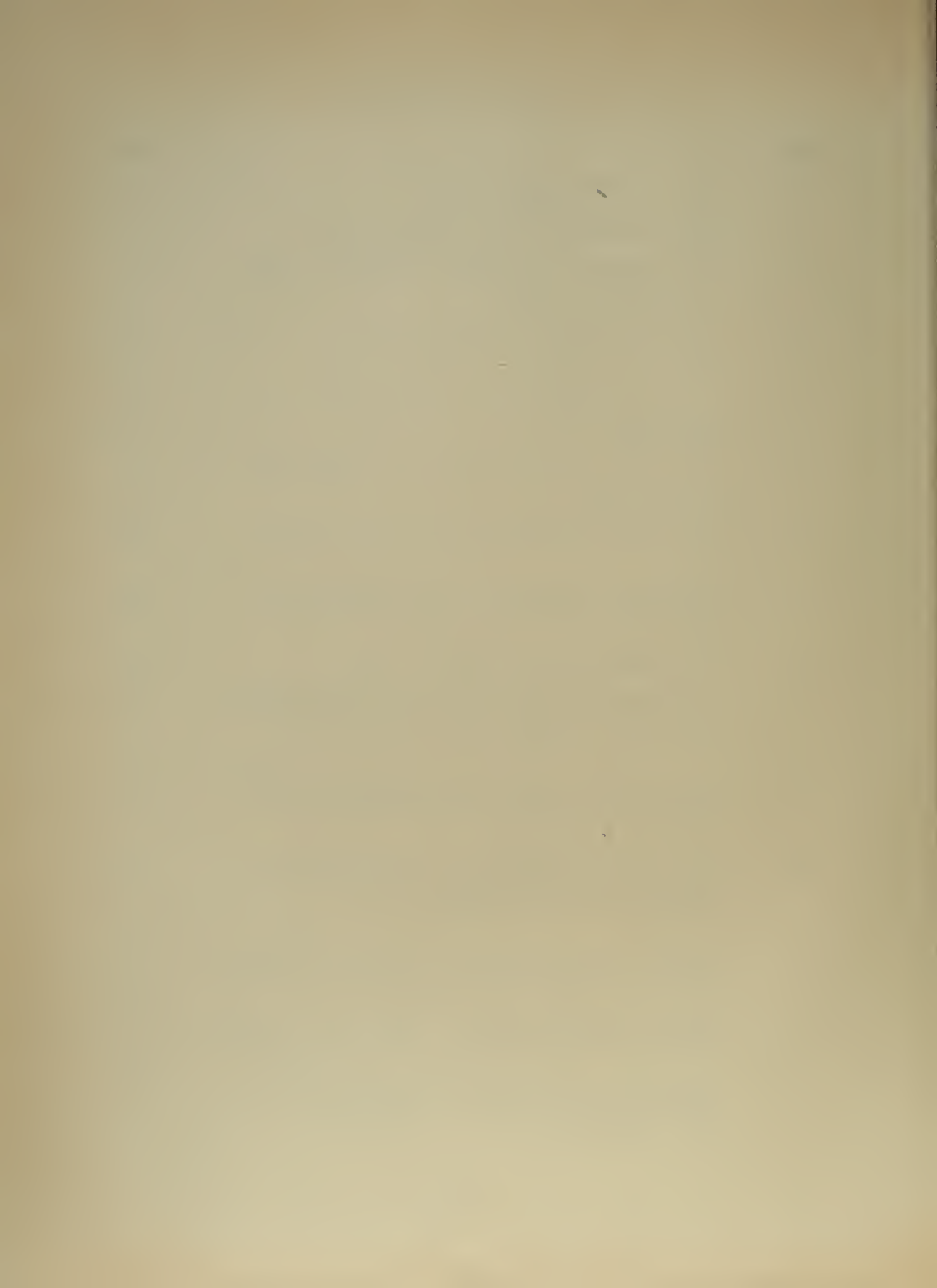
The writer wishes to express his appreciation for the assistance and encouragement given him in this investigation by Professors Lawrence E. Kinsler and Herman Medwin of the U. S. Naval Postgraduate School and Dr. T. F. Hueter of Raytheon Manufacturing Company, under whose guidance the actual research was carried out.

TABLE OF CONTENTS

Section	Title	Page
1.	Introduction	1
2.	Barium Titanate as a Transducer Material	2
3.	Recently Developed Ferroelectrics	3
4.	Composition of Lead Zirconate Titanate	5
5.	Preparation of Specimens	7
5.1.	Firing of Specimens	8
6.	Measurements Program	8
6.1.	Materials Used	9
6.2.	Piezoelectric Measurements	9
6.3.	Loss Measurements	15
6.4.	Polarization Study	15
7.	Test Results	21
7.1.	Piezoelectric Properties	21
7.2.	Loss Factor Studies	22
7.3.	Polarizing Studies	22
8.	Conclusions	25
9.	Bibliography	53

LIST OF ILLUSTRATIONS

Figure		Page
1.	Cubic Perovskite-type Structure	5
2.	Phase Diagram of PbZrO_3 - PbTiO_3 System	6
3.	Radial Coupling Coefficient for PbTiO_3 - PbZrO_3 Solid Solution Ceramics	7
4.	Admittance Diagram in Air of PZT-4 Disc	13
5.	Admittance Diagram in Air of PZT-5A Disc	14
6.	Polarization Procedures A & B, Temperature vs Time Curves	17
7.	Polarization Procedures C, D, & E, Temperature vs Time Curves	17
8.	Polarization Procedure F, Temperature vs Time Curve	18
9.	Polarization Procedures G & H, Temperature vs Time Curves	18
10.	Block Diagram of Pulsed Sound System	20
11.	Radial Coupling Coefficient, Transverse Coupling Coefficient and Piezoelectric Coefficients vs Temperature of PZT-4	26
12.	Radial Coupling Coefficient, Transverse Coupling Coefficient and Piezoelectric Coefficients vs Temperature of PZT-5A	27
13.	Radial Coupling Coefficient, Transverse Coupling Coefficient and Piezoelectric Coefficients vs Temperature of $\text{Pb}(\text{Zr}_{.55}\text{Ti}_{.45})\text{O}_3$	28
14.	Dielectric Constant, Young's Modulus, Frequency Constant and Mechanical Q vs Temperature of PZT-4	29
15.	Dielectric Constant, Young's Modulus, Frequency Constant and Mechanical Q vs Temperature of PZT-5A	30
16.	Dielectric Constant, Young's Modulus, Frequency Constant and Mechanical Q vs Temperature of $\text{Pb}(\text{Zr}_{.55}\text{Ti}_{.45})\text{O}_3$	31



LIST OF ILLUSTRATIONS (Continued)

Figure		Page
17.	Loss Factor vs Temperature with A.C. Field as a Parameter of PZT-4	34
18.	Loss Factor vs Temperature with A.C. Field as a Parameter of PZT-5A	35
19.	Loss Factor vs Temperature with A.C. Field as a Parameter of $\text{Pb}(\text{Zr}_{.55}\text{Ti}_{.45})\text{O}_3$	36
20.	Loss Factor vs A.C. Field with Temperature as a Parameter of PZT-4	37
21.	Loss Factor vs A.C. Field with Temperature as a Parameter of PZT-5A	38
22.	Loss Factor vs A.C. Field with Temperature as a Parameter of $\text{Pb}(\text{Zr}_{.55}\text{Ti}_{.45})\text{O}_3$	39
23.	Dielectric Constant vs A.C. Field with Temperature as a Parameter of PZT-4	40
24.	Dielectric Constant vs A.C. Field with Temperature as a Parameter of PZT-5A	41
25.	Acoustic Output vs Electric Input of PZT Discs Polarized by Various Procedures	42
26.	Frequency of Radial Resonance vs Radial Coupling Coefficient Squared of PZT-4 Discs	44
27.	Percent change in Frequency of Radial Resonance Due to Polarization vs Radial Coupling Coefficient Squared of PZT-4 Discs	45
28.	Admittance Diagram in Water of PZT-4 Transducer "B"	46
29.	Admittance Diagram in Water of PZT-4 Transducer "C"	47
30.	Admittance Diagram in Water of PZT-4 Transducer "D"	48
31.	Admittance Diagram in Water of PZT-4 Transducer "E"	49
32.	Admittance Diagram in Water of PZT-4 Transducer "F"	50
33.	Admittance Diagram in Water of PZT-4 Transducer "G"	51
34.	Admittance Diagram in Water of PZT-4 Transducer "H"	52



LIST OF ILLUSTRATIONS (Continued)

Table		Page
I	Comparison of Published Data on PZT and Barium Titanate, 20°C	4
II	Comparison of Measured Piezoelectric and Dielectric Properties of Lead Zirconate Compositions with Published Data of Barium Titanate, 20°C	32
III	Maximum Percentage Change of PZT Compositions in the Temperature Range from 20°C to 120°C	33
IV	Results of Polarizing Procedures of PZT-4	43

1. Introduction.

The active elements for converting electrical energy into mechanical energy, and vice versa, in acoustic transducers utilize either magnetostrictive or piezoelectric effects. Magnetostrictive materials used include nickel, Permendur and some ferrites. Piezoelectric materials fall into two main classes, piezoelectric¹ crystals such as quartz and ferroelectric² crystals which may be grouped into four families on crystal-chemical basis. The first to be discovered was Rochelle Salt (R.S.) which is a member of the tartrate family. Next discovered were the alkali metal dihydrogen phosphates and arsenates represented by potassium dihydrogen phosphate (KDP) and ammonium dihydrogen phosphate (ADP). The third class of ferroelectrics is entitled the oxygen-octahedra family, on the basis of their crystal structure. This family includes the very important sub-group of perovskite-type ferroelectrics whose structures are slight distortions of that of the mineral perovskite, CaTiO_3 . The best known member of this sub-group is barium titanate, BaTiO_3 , but the number of ferroelectrics to be found among perovskite-type crystals is tremendously large. Finally, the latest family to be discovered is a new and unrelated type represented by guanidine aluminum sulfate hexahydrate (GASH), whose structure has not yet been determined.

¹Piezoelectricity is defined as "electric polarization produced by mechanical strain [and conversely] in crystals belonging to certain classes, the polarization being proportional to strain and changing sign with it." (see [7], page 4)

²A ferroelectric crystal is defined as "a crystal which exhibits a spontaneous electric dipole moment; in other words, a crystal for which even in the absence of an applied electric field the center of positive charge does not correspond with the center of negative charge. All ferroelectrics will be piezoelectric, but not all piezoelectrics will be ferroelectric (e.g., quartz)." (see [23], page 182)

Quartz exhibits a first order piezoelectric effect in which the relation between strain and electric displacement is linear. A second order piezoelectric effect is present in all other crystals (including solid insulators) in which the strain is proportional to the square of the electric displacement. Compared to the first order, or piezoelectric phenomena, the second order, or electrostrictive effects, are usually extremely small except in ferroelectric materials. Barium titanate and a recently developed material, lead zirconate titanate (PZT), are two such materials which exhibit a large electrostrictive effect.

2. Barium Titanate as a Transducer Material.

The excellent electroacoustic and mechanical properties of the ferroelectric materials have encouraged their almost exclusive use in current practical applications. Since barium titanate ceramics can be readily fabricated in a great variety of shapes and structures, they are in wide use in all types of ultrasonic transducers, sensing devices, and hydrophones.

Barium titanate ceramics, however, may be utilized only in applications not requiring extreme temperature or time stability. Barium titanate exhibits three different ferroelectric phases with transition points at -80°C , 5°C and 120°C . At the transition points, the various piezoelectric properties exhibit large peaks or dips, while in the interval between the transition points, the piezoelectric properties often change rapidly with temperature.

Compositional additives, such as calcium, lead and strontium have proved useful in improving temperature stability within given temperature regions. Unfortunately, additives which provide high temperature stability cause lowered electromechanical coupling; in general, the better the temperature stability, the lower the coupling.

A more serious design limitation of barium titanate transducers, however, is their low power handling capacity. Below its Curie Point of 120°C , barium titanate has the ability to retain electromechanical activity after application of a polarizing field. It has been observed that under large a.c. fields such as are applied in ultrasonic and high power applications, this polarization and thereby the electromechanical activity may be appreciably reduced or virtually lost. This is partly due to direct polarization as the opposing peak charge density becomes an appreciable fraction of the originally retained polarization and partly due to the temperature increase caused by rapidly increasing dielectric losses.

It has recently been found that the addition of small amounts of Cobalt to certain barium titanate mixtures produces a significant reduction in the dielectric loss without appreciably reducing the electromechanical activity. The resultant gain in power handling capacity is important to note.

3. Recently Developed Ferroelectrics.

Recently several other ferroelectric materials have been found which have the ability to retain electromechanical activity when polarized. In particular, several compositions of lead zirconate titanate appear to have promise in the areas in which barium titanate has been found lacking, namely high temperature and high power applications. The properties of PZT are compared with those of barium titanate in Table I. It may readily be seen that the published properties of PZT are particularly outstanding.

TABLE I

Comparison of Published Data on PZT and Barium Titanate, 25°C [3]

	Planar Coupling K_T	Dielectric Constant ϵ	Strain Field d_{31} $\times 10^{-12}$ meter/volt	Force Field E_{31} $\times 10^{-3}$ volt./newton	Elastic Modulus Y $\times 10^9$ newton/m ²	Freq. Constant cycle·m	Mechanical Quality Q_M	Curie Point °C	Density $\times 10^3$ kg/m ³
Barium Titanate									
Brush Ceramic B	.33	1200	-58	-5.5	116	2300	500	113	5.5
$Pb(Zr_{.55}Ti_{.45})O_3$									
Nat.Bu. Standards	.37	500	-50	-11	75	1550	100	350	7.1
PZT									
Brush Labs*	.48	850	-96	-12.7	83	—	—	~300	7.64

*The superior results obtained by the Brush Laboratory are presumably due to addition of small amounts of various elements to $Pb(Zr_{.55}Ti_{.45})O_3$ and/or to a slight variation of percentages of zirconium and titanium in the $Pb(Zr,Ti)O_3$ system.

4. Composition of Lead Zirconate Titanate.

Lead titanate is a perovskite-type ferroelectric, similar in crystalline structure to barium titanate. The perovskite structure is the simplest crystal structure, ABO_3 , in which the A ions occupy the corners, the B ions occupy the center position of a unit cell, with the oxygen ions at the center faces (see Figure 1). The ferroelectric compounds have been found to have either rhombohedral, tetragonal or orthorhombic symmetry. (See Figure 1).

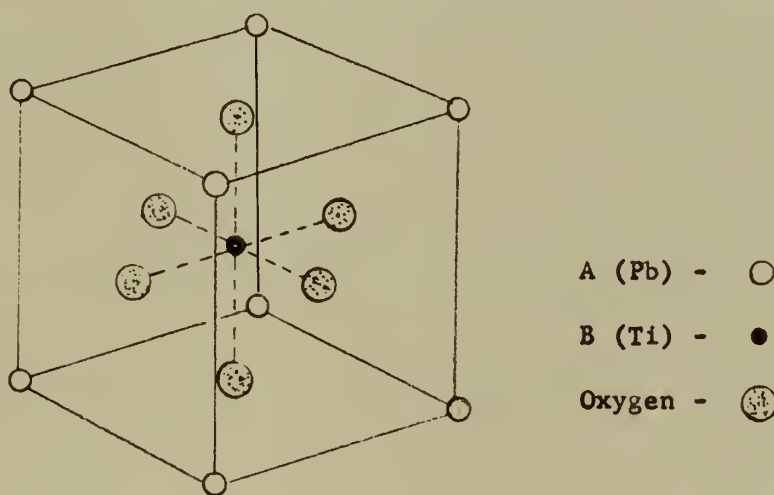


Figure 1. Cubic perovskite - type structure - ABO_3

Lead zirconate, reported by Roberts [32] to have a tetragonal perovskite-type structure, is considered to be antiferroelectric and therefore cannot be polarized to exhibit a piezoelectric effect. In 1952, the properties of the $PbZrO_3$ - $PbTiO_3$ system were described by Shirane, Suzuki and Takeda [41, 42, 43] and were later reviewed by Sawaguchi [34]. It was found that lead zirconate becomes ferroelectric in the presence of 10 mole % or more of lead titanate. The phase diagram

of the system PbZrO_3 - PbTiO_3 as determined by Sawaguchi [34] is shown in Figure 2.

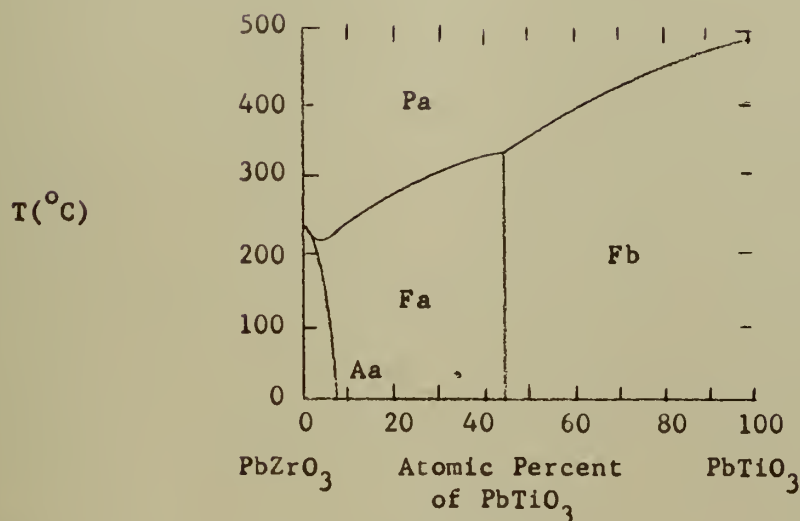


Figure 2. Phase diagram of PbZrO_3 - PbTiO_3 system. Pa - paraelectric, cubic; Fa - Ferroelectric, rhombohedral; Fb - ferroelectric, tetragonal; A - antiferroelectric (After Sawaguchi [34])

A morphotropic¹ phase boundary occurs at about 45 mole % lead titanate. Solid solutions containing less than 45 mole % lead titanate are rhombohedral, while those containing more than this amount are tetragonal, isostructural with both lead titanate and barium titanate.

The optimum percentages of PbTiO_3 and PbZrO_3 to be used in the $\text{Pb}(\text{Zr},\text{Ti})\text{O}_3$ system may be determined from Figure 3. The electromechanical response of the rhombohedral specimens increases sharply as the transition composition at 45 mole % is approached. The tetragonal compositions nearest the boundary also have strong response. However, still more lead titanate causes a marked decrease, and ceramics containing 60

¹A morphotropic transformation is an abrupt change in structure of a solid solution with variation in composition.

mole % or more of lead titanate show no electromechanical activity after polarization.

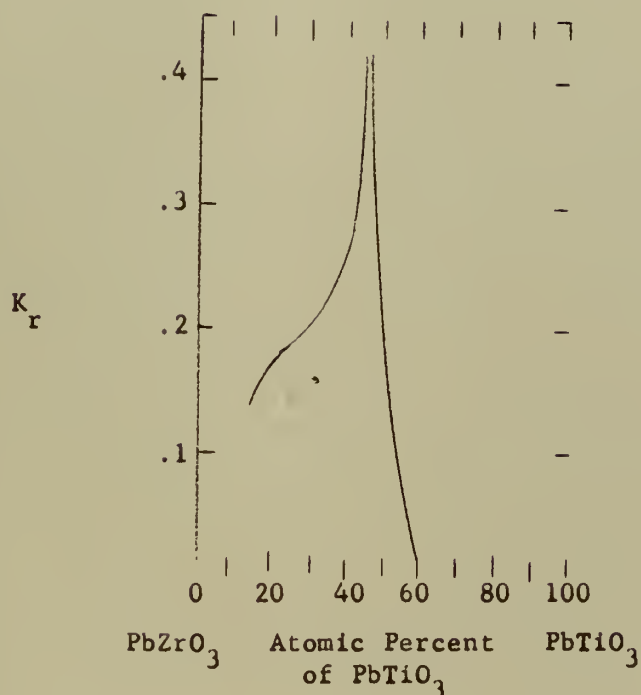


Figure 3. Radial Coupling Coefficient (K_r) for PbTiO_3 - PbZrO_3 solid solution ceramics. (After Jaffe et. al. [20])

5. Preparation of Specimens.

The materials used to prepare samples of PZT include reagent grade PbO , a commercially pure grade of ZrO_2 , and a good dielectric grade of TiO_2 . The ingredients are weighed and ball milled with distilled water for intimate mixing. The mix is dried, mixed again in a mortar, and calcined at $800^\circ - 850^\circ\text{C}$ in a covered alumina or platinum crucible.

The calcined mix is then ground thoroughly and specimens pressed into desired shape in steel dies at pressures of 10,000 - 15,000 psi.

5.1. Firing of Specimens.

Since the lead oxide in lead zirconate and its solid solutions is volatile, its loss can only be controlled by firing the specimens in an atmosphere that contains lead oxide vapor. One method of accomplishing this is to place pellets of $\text{PbO} + \text{ZrO}_2$ enriched in PbO in the crucible with the specimens. The pellet provides an "atmosphere" enriched in PbO vapor to retard evaporation of the specimens. The weight of the "atmosphere" pellet is critical, for it has been found that the final weight of the specimens can be controlled by the "atmosphere" pellet.

The joints of the crucible may be sealed with a TiO_2 paste or the crucible may be placed in a larger furnace which also contains an "atmosphere" pellet. The specimens are then fired by heating at a uniform rate up to the soaking temperature which is in the order of $1200 - 1300^\circ\text{C}$. After soaking the specimens for 20 - 60 minutes, the furnace is allowed to cool naturally.

6. Measurement Program.

An investigation of lead zirconate titanate was conducted at the Wayland Laboratory of the Raytheon Manufacturing Company in order to ascertain its potential for use in sonar transducers and hydrophones. The program included:

- a. Studies of piezoelectric properties at low level including coupling coefficient and loss factor as a function of temperature.
- b. Studies of loss factor as a function of drive level.
- c. Studies of suitable polarizing techniques, and polarizing field as a function of time of application and temperature.

6.1. Materials Used.

Several compositions of lead zirconate titanate were tested, two types, PZT4 and PZT-5A, prepared by Brush Laboratories of Cleveland, Ohio,

and one type, $\text{Pb}(\text{Zr}_{.55}\text{Ti}_{.45})\text{O}_3$ (laboratory samples roughly corresponding to the National Bureau of Standards mixture [17]) prepared by the Research Division of Raytheon Manufacturing Company, Waltham, Massachusetts. The physical dimensions of the specimens are listed below:

Type	Diameter (inches)	Thickness (inches)
*PZT-4	1	0.75
PZT-4	1	.095
PZT-5A	1.75	.1
$\text{Pb}(\text{Zr}_{.55}\text{Ti}_{.45})\text{O}_3$	1.75	.12

*After measurements were made on the thick discs of PZT-4, they were then sliced, electroded, and repolarized for further study as thin discs.

All of the measurements of the piezoelectric properties of PZT-4 and $\text{Pb}(\text{Zr}_{.55}\text{Ti}_{.45})\text{O}_3$ are averages of two or more specimens. The piezoelectric properties of PZT-5A are single disc values.

The data obtained on polarizing techniques of PZT-4 are also single disc values.

6.2. Piezoelectric Measurements.

The chief figure of merit often used to evaluate the piezoelectric properties of a ceramic is the radial coupling coefficient.¹ Thin discs vibrating at radial resonance present an isolated resonant mode which may be accurately measured. The radial coupling factor may be conveniently calculated from the measured resonant and anti-resonant frequencies, using the following equation, adapted from Mason [26]:

¹Coupling coefficient - "k" - a dimensionless quantity defined as the square root of the ratio of mechanical energy stored in the crystal to the electric energy absorbed by the crystal; it is a true measure of the efficiency of the crystal as a transducer or converter of energy.

$$k_r^2 = \frac{2.51 \frac{\Delta F}{F_r}}{1 + 2.51 \frac{\Delta F}{F_r}}$$

F_r = Resonant frequency, Kcs.

F_a = Antiresonant frequency, Kcs.

$$\Delta F = F_a - F_r$$

The resonant frequency was determined by varying the frequency of a Western Electric 17B oscillator, acting as a constant current source through a 1000 ohm resistance, for a minimum impedance (voltage) of the specimen.

The antiresonant frequency was obtained by varying the frequency for maximum impedance (voltage) of the specimen at constant current through a 500K ohm resistance. Frequency was measured with a Potter 840 Frequency Counter; voltage was measured with a Hewlett Packard 400A VTVM.

From the measured radial coupling coefficient and Poisson's ratio, the transverse coupling factor may be determined:

$$k_{31}^2 = \frac{1 - \sigma}{2} k_r^2$$

σ = Poisson's ratio, taken as .3

k_{31} = transverse coupling coefficient

Young's modulus of elasticity may be determined as follows [26]:

$$Y_o^E = \left[\frac{2\pi a F_r}{2.03} \right]^2 \left[\rho (1 - \sigma^2) \right]$$

Y_o^E = elastic modulus, $\frac{\text{newton}}{\text{meter}^2}$

a = disc radius, meters

ρ = density, $\frac{\text{kilograms}}{\text{meter}^3}$

The radial mode frequency constant of the material is:

$$FC = F_r d$$

FC = frequency constant, cycles meter

d = disc diameter, meters

Piezoelectric ceramic elements have two main uses, one as a generator of mechanical energy (ultrasonic generator or loudspeaker), and the other as a generator of an electrical signal (phonograph pickup or hydrophone).

For the first use, a high "d" constant¹ is important; for the second, a high "g" constant² is desired. Thus, although the coupling coefficient is a valid figure of merit, high "d" and "g" are individually desirable for most applications. The d and g coefficients were calculated from the following relations:

$$d_{31} = k_r \sqrt{\frac{(1 - \sigma) \epsilon_0 \epsilon}{2Y_o^E}}$$

d_{31} = transverse piezoelectric constant $\frac{\text{coulombs}}{\text{newton}}$

ϵ_0 = permittivity of vacuum (8.86×10^{-12} farads/meter)

ϵ = relative dielectric constant at 25°C and at a frequency below all resonances (1 kc)

$$g_{31} = \frac{d_{31}}{\epsilon_0 \epsilon}$$

g_{31} = transverse piezoelectric constant $\frac{\text{meter volts}}{\text{newton}}$

The blocked capacitance and loss factor³, $\tan \delta$, at 1 kc of the specimens were measured directly with a General Radio 716-C Capacitance Bridge

¹"d" coefficient is the basic coefficient long used by crystal physicists; it gives the ratio of electric charge density output per unit pressure input under short circuit conditions, and conversely the deformation obtained per unit applied voltage under no load conditions. It may therefore be called the piezoelectric compliance coefficient and in the MKS system is measured in: $\frac{\text{coulombs}}{\text{newton}}$ or $\frac{\text{meters}}{\text{volt}}$ [8]

²"g" coefficient - a measure of the e.m.f. gradient per unit pressure applied obtained by dividing the "d" constant by the free dielectric constant (8.86×10^{-12} farads/m). It may be termed the elasto-electric coefficient and is measured in $\frac{\text{meter-volts}}{\text{newton}}$ [8]

³The loss factor, $\tan \delta$, is defined as the ratio of the loss rate to the stored energy rate.

$$\tan \delta = \frac{1}{\omega R_e C_o}$$

R_e = electrical resistance, ohms

C_o = blocked capacitance, microfarads

ω = radians/sec at desired frequency

which uses a modified Schering bridge circuit. A Hewlett Packard 200C Audio Oscillator, set at 1 kc was used as generator and a Ballantine 801 VTVM was used as the detector.

The free dielectric constant of the specimen may then be computed from the expression for a parallel plate condenser:

$$\epsilon = \frac{36\pi t C_o \times 10^5}{A}$$

ϵ = free dielectric constant (at 1 kc)

t = thickness of disc, centimeters

A = area of disc, centimeters²

C_o = blocked capacitance of disc, microfarads

Admittance measurements vs frequency were taken on the specimens using a precision admittance (parallel impedance) bridge¹, a Western Electric 17B oscillator and a Potter 840 Frequency Counter. The mechanical Q of the disc may be obtained from the admittance vs frequency circle:

$$Q_m = \frac{F_2 - F_1}{F_r}$$

Q_m = mechanical Q

F_2, F_1 = frequencies of half power points.

The radial coupling factor may also be obtained from the admittance circle using the following formula, adapted from Mason [26]:

$$k_r^2 = \frac{D_A}{\frac{8}{\pi^2} B_e Q_m + D_A}$$

D_A = diameter of admittance circle, mhos

B_e = blocked susceptance, mhos

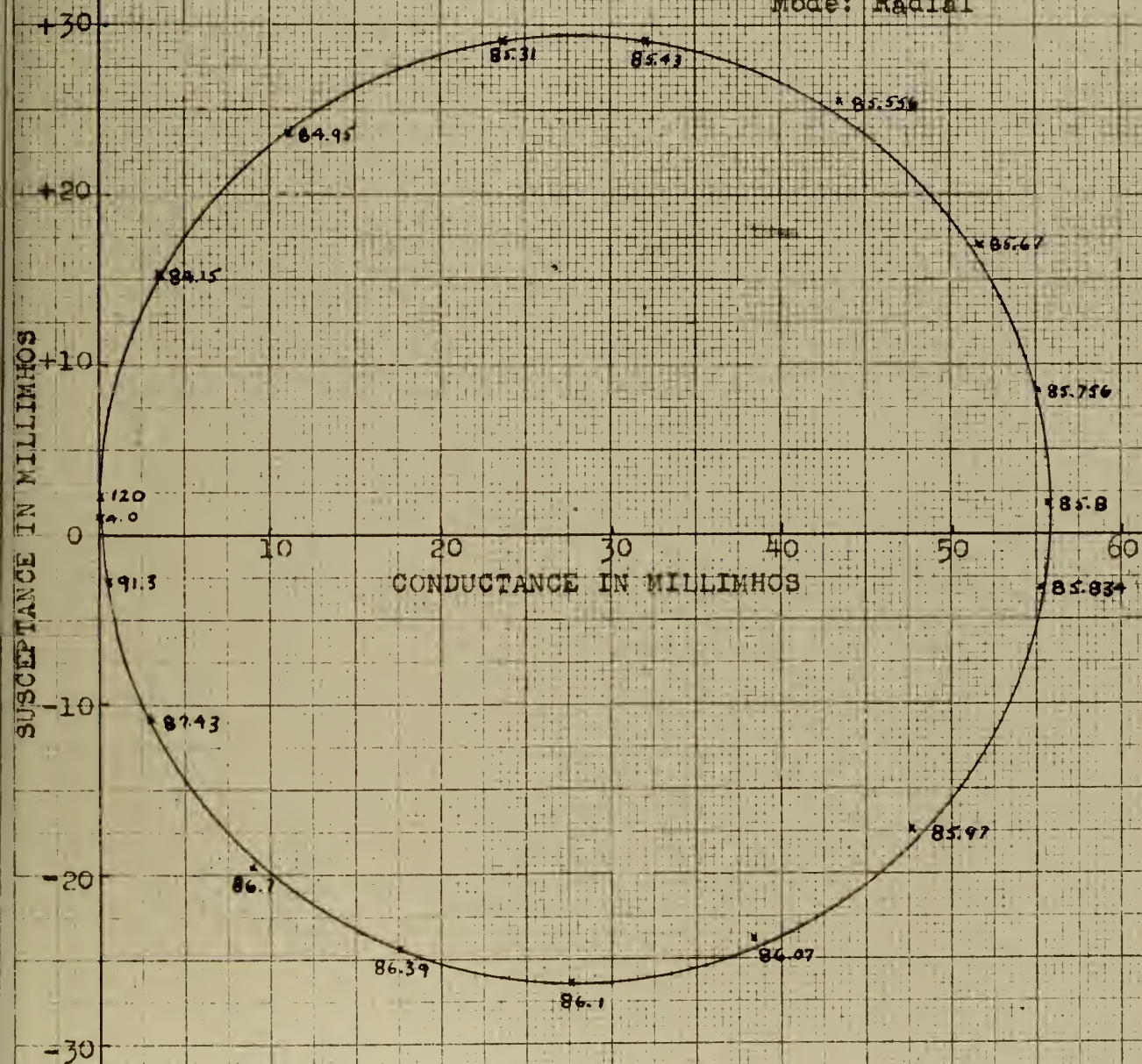
Figures 4 and 5 present the typical admittance versus frequency circles in air at room temperature for unloaded discs of PZT-4 and PZT-5A.

¹This bridge resembles the Harvard Underwater Sound Laboratory Bridge [29] except for the addition of a Submarine Signal Company tuned R.F. amplifier and null detector, and some special shielding. It covers the frequency range from 1-150 kc with an accuracy of better than .5%.

ADMITTANCE IN AIR OF LEAD ZIRCONATE TITANATE DISC

FIG. 4

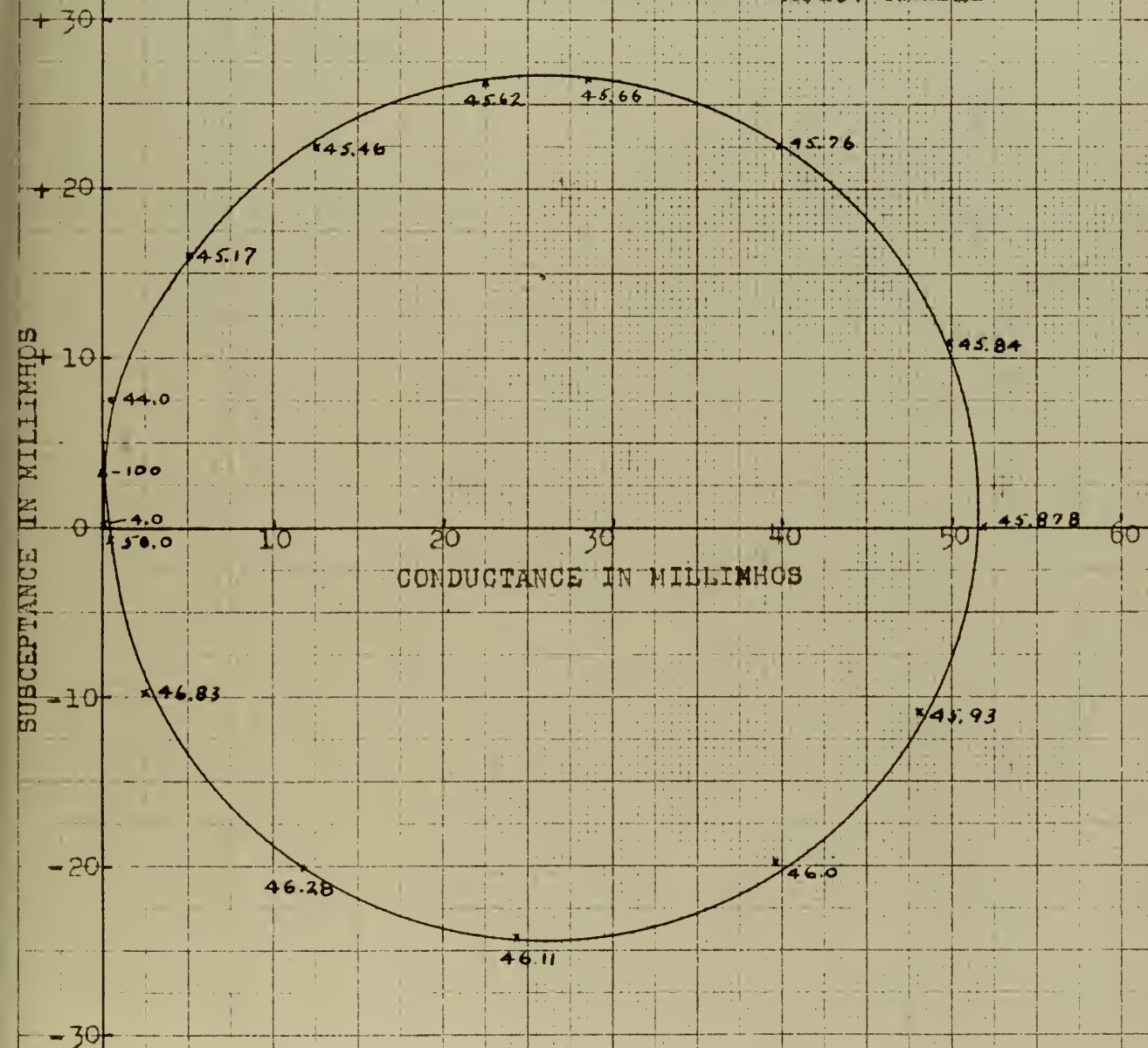
Material: Brush PZT-4
Diameter: 1 inch
Thickness: 0.051 inch
Temperature: 20°C
Mode: Radial



ADMITTANCE IN AIR OF LEAD ZIRCONATE TITANATE DISC

FIG. 5

Material: Brush PZT-5A
 Diameter: 1.77 inch
 Thickness: 0.1 inch
 Temperature: 20°C
 Mode: Radial



Measurements were taken over a temperature range of 15°C to 200°C which generally exceeds the expected temperatures to be encountered in use or in storage. Temperature runs were taken with the specimens in an oven or a silicone oil bath, as was deemed appropriate. All readings were taken with the temperature rising slightly to avoid relaxation or hysteresis phenomena.

6.3. Loss Measurements.

Baerwald [1] has shown that for moderate losses, capacitance bridge methods may be justified for loss factor measurements. Consequently, to measure loss factor as a function of drive level a General Radio 716-B Capacitance Bridge was used with a Communications Measurement Laboratory Model 1425C Variable Frequency Electronic Generator set at 1 kc and a Ballantine 813 VTVM as detector.

6.4. Polarization Study.

Due to its relatively high Curie temperature of approximately 350°C, the polarization problems for PZT are presumably different from those for barium titanate materials. An investigation was therefore conducted to evaluate the effectiveness of cold versus hot polarization and the optimization of polarization techniques; i.e., temperature, time and voltage relationships.

The effect of time on cold polarization was first considered. Specimens were polarized at room temperature in a Silicone oil bath¹ at 40 KV/cm for 2 and 4 hours. (See Figure 6). These were designated specimens A and B respectively.

In order to establish the effect of field strength on polarization, three identical time vs temperature procedures were conducted. (See

¹Dow Corning 550 Silicone Fluid.

Figure 7). In all cases the temperature was raised to 100°C , held for an hour and allowed to cool slowly to room temperature. Polarizing voltage was applied when the temperature reached 50°C . Procedure C had a field strength of 40 KV/cm, procedure D had a field strength of 30 KV/cm, and procedure E had a field strength of 20 KV/cm.

In order to ascertain the effect of polarizing at high temperature, approaching the Curie point of PZT, procedure F was tried. (See Figure 8). The specimen was heated to 200°C , held for 30 minutes and allowed to cool slowly to room temperature. The polarizing voltage of 20 KV/cm was applied when the temperature reached 50° . However, due to the decrease of d.c. resistance of the ceramic with increasing temperature, the output voltage of the power supply decreased as the d.c. resistance of the ceramic approached the output impedance of the power supply. Consequently, at 200°C , the effective polarizing voltage across the sample was in the order of 3 KV/cm.

The effect of time on hot polarization was also considered. (See Figure 9). In procedure G, using a field strength of 40 KV/cm the specimen was heated to 100°C , the heat source was removed, and the specimen was allowed to cool slowly to room temperature. This procedure shortened the time of procedure D by one hour. Finally, procedure H was suggested by analysis of the results of previous runs. Again using a field strength of 40 KV/cm, the specimen was heated quickly to 100°C and then more slowly until the d.c. current through the power supply began to increase rapidly at which point the polarizing voltage began to decrease. The heat source was then removed and the specimen allowed to cool slowly to room temperature.

Two types of tests were used to evaluate the above mentioned polarization procedures.

POLARIZATION PROCEDURES

TEMPERATURE vs. TIME

FIG. 6

Lead Zirconate Titanate
Brush PZT-4

Procedure	Field Strength
A	40 kv/cm
B	40 kv/cm

TEMPERATURE vs. TIME

FIG. 7

Lead Zirconate Titanate
Brush PZT-4

Procedure	Field Strength
C	40 kv/cm
D	30 kv/cm
E	20 kv/cm

TEMPERATURE - °C

TIME - hours

POLARIZATION PROCEDURES

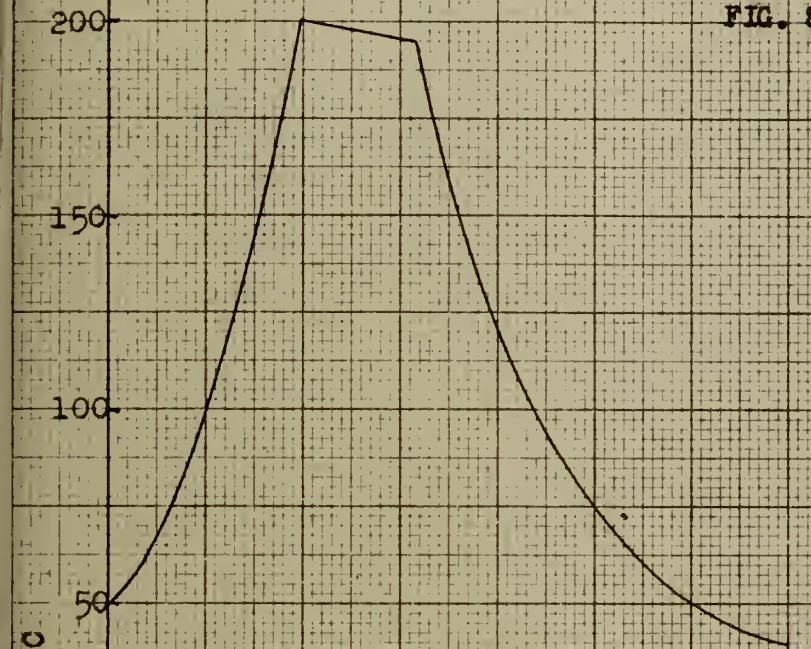
TEMPERATURE vs. TIME

FIG. 8

Lead Zirconate Titanate
Brush PZT - 4

Procedure
F

Field Strength
20 kv/cm



TEMPERATURE vs. TIME

FIG. 9

Lead Zirconate Titanate
Brush PZT-4

Procedure

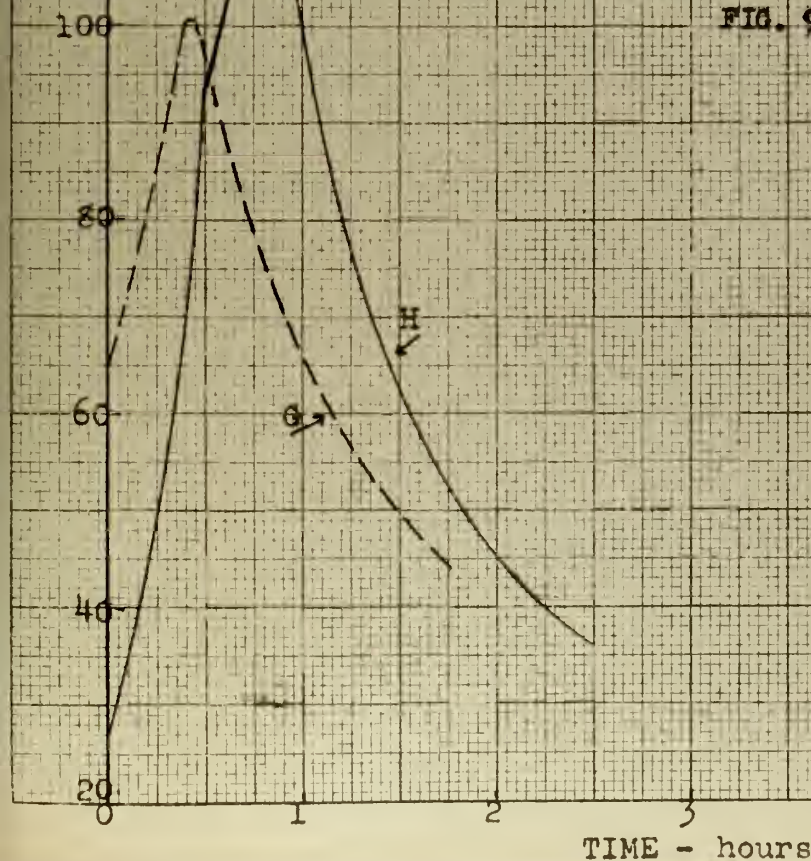
Field Strength

G

40 kv/cm

H

40 kv/cm

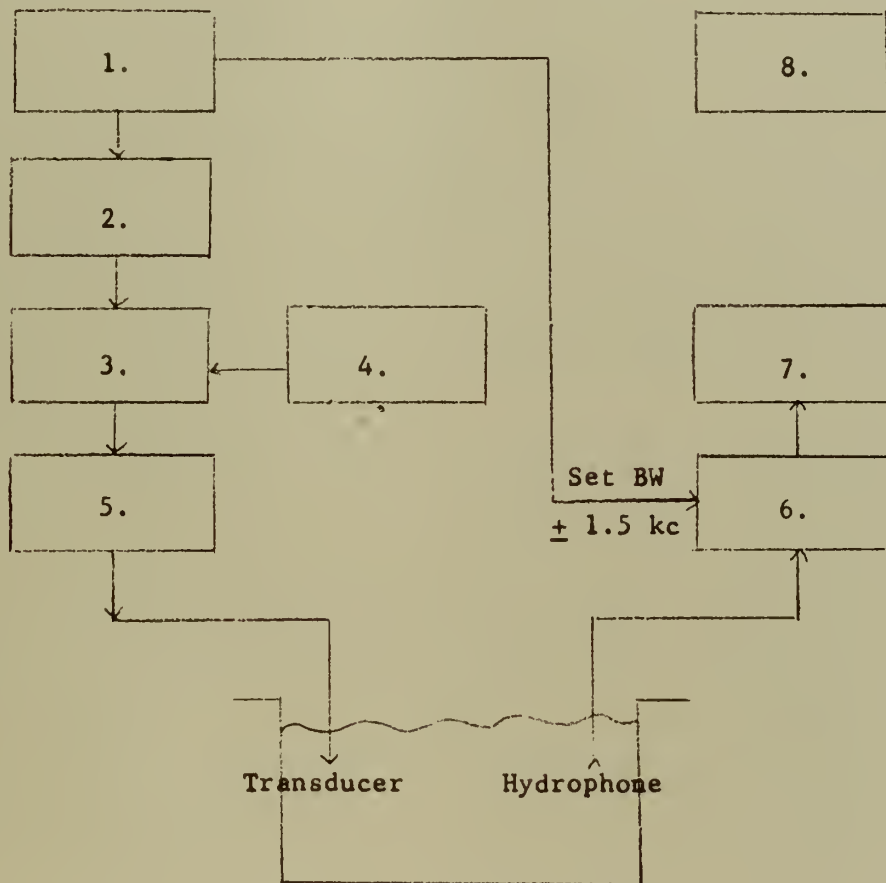


(1) Determination of radial coupling coefficient from measurement of resonant and antiresonant frequencies, and

(2) Evaluation of the specimen as a transducer element; i.e., response tests in water of acoustic output vs electrical input for low to medium level power inputs.

For the latter tests, the specimens were cemented to a backing plate and placed in a transducer housing. The transducer was placed in a large test tank (24 x 12 x 13 feet) and a Massa Laboratories type M115-B calibrated hydrophone located one meter from the transducer. Since standing waves were found to be present in the tank when a continuous wave oscillator was used to drive the transducer, a pulsed-sound technique was used for all measurements. (See Figure 10 for the block diagram of equipment arrangement). The hydrophone response was fed to gating circuits, and all reflected pulses were gated out. The oscillator was tuned to the resonant frequency of the transducer (as determined from the admittance circle in water) and acoustic output observed as electrical input power was varied. Electrical input was determined from measured values of input voltage and input current and values of phase angle computed from admittance measurements. Acoustic output in db re 1 volt/dyne/cm² was observed directly on a calibrated detector.

Figure 10. Block Diagram of Pulsed Sound System.
Raytheon Automatic Transducer Calibrator (Raytrac)



1. Oscillator, Techno Instrument Co., Type TI-213
2. Send Modulator, Techno Instrument Co., Type TI-214
3. Transmitter Gate, Raytheon Manufacturing Company
4. Pulse Generator, Raytheon Manufacturing Company
5. Power Amplifier, Raytheon Manufacturing Company
6. Receiver, Raytheon Manufacturing Company
7. Power Level Recorder, Leeds & Northrup Co.
8. Cathode Ray Oscilloscope, Tektronix Type 512

7. Test Results.

7.1. Piezoelectric Properties.

The variation of radial coupling coefficient (k_r), transverse coupling coefficient (k_{31}), d_{31} constant, g_{31} constant, free dielectric constant (ϵ), Young's modulus (Y_{11}^E), frequency constant (FC), and mechanical Q (Q_m) from 0°C to 180°C of the three lead zirconate compositions studies are plotted in Figures 11 through 16. It is particularly noteworthy that the coupling coefficients and frequency constant are extremely stable over a wide temperature range and the remaining quantities do not change greatly, percentage wise.

Table II compares the above quantities at 20°C with published data for barium titanate Ceramic B. It should be pointed out that the specimens of $\text{Pb}(\text{Zr}_{.55}\text{Ti}_{.45})\text{O}_3$ were laboratory samples and hence not representatives of commercially produced materials. The samples were apparently not homogeneous, or impurities were present, for the polarizability was low, which led to low values for the coupling coefficient and the values derived therefrom. The data of PZT-4 and 5A indicate that when techniques of manufacture have been mastered, the properties of PZT are outstanding. The coupling coefficients, d_{31} constant, and g_{31} constant are 60 to 100% greater than those of Ceramic B. The low value of dielectric constant listed in Table I for $\text{Pb}(\text{Zr}_{.55}\text{Ti}_{.45})\text{O}_3$ has been increased by compositional additives in PZT-4 and 5A to a value comparable to that of Ceramic B and the loss factors are, in general, lower than that of Ceramic B. The lower values of Young's modulus and frequency constant recorded for PZT indicate that for a given frequency, the size of the active elements (and thereby the transducer housing) may be smaller than those of Ceramic B which is indeed fortunate in view of the

increased density of PZT. Finally, the high Curie point of PZT leaves no doubt as to its superiority over barium titanate in high temperature applications.

Table III lists the maximum percentage change with respect to the values at 20°C of the piezoelectric properties of PZT in the temperature range from 20°C to 120°C. The relatively small percentage changes are even more impressive when it is realized that barium titanate ceramics are no longer piezoelectric at 120°C.

7.2. Loss Factor Studies.

The variation of $\tan \delta$ with both temperature and driving field for the three lead zirconate compositions are plotted in Figures 17 through 22. In all cases it was found that the electrical losses of the PZT compositions increase but slowly with temperature. The curves of $\text{Pb}(\text{Zr}_{.55}\text{Ti}_{.45})\text{O}_3$ and PZT-4, in addition, show low loss factors with large driving fields. Figures 18 and 21 indicate that PZT-4 is particularly well suited to high power-high temperature applications without fear of high dielectric losses and resultant depolarization.

The variation of dielectric constant with both temperature and driving field for PZT-4 and 5A is plotted in Figures 23 and 24. It is noted that the dielectric constant increases with both temperature and drive level, although not severely so. In a transducer this would be reflected as an impedance change which would have to be allowed for.

7.3. Polarizing Studies.

The results of the polarizing procedures previously described are presented graphically in Figure 25 and in tabular form in Table IV and it is seen that the results, in general, agree.

Curves A and B indicate that cold polarization at 40 KV/cm is not a very practical procedure. To polarize successfully at room temperature high field strengths in the order of 60 KV/cm are required. However, high field strengths prove hazardous to specimens that are flawed or inhomogeneous, and the percentage of breakages and breakdowns in production quantities might be too large to tolerate.

Curves C, D and E indicate that moderately high field strengths are required even at 100°C. In each case the time-temperature curves are identical and only the field strength is varied. At 100°C a field strength of 40 KV/cm is clearly superior to lower field strengths.

Curve F seems to indicate that too high a temperature may be detrimental to polarization, even at lowered field strengths. In a polarization study of barium titanate, Froemel [9] reported that barium titanate reduces quite easily, especially at high field strengths and temperatures. Reduction causes an increase in conductivity with a resultant loss of permanent polarization. When this occurs the area becomes more conductive and the extent of conduction can be measured by the change in capacitance after polarization. Apparently the mechanism of reduction occurs in a similar manner in PZT-4 since not only was the resultant polarization low, but the increase in dielectric constant of sample F was completely out of proportion to that of the other samples.

Curve G evaluates the result of decreasing the time of hot polarization. Comparison of curves C and G indicates that nothing is to be gained by holding the temperature at 100° for any length of time.

Procedure H was an attempt to optimize procedure G. Although the radical coupling coefficient of H is the highest obtained, it should be noted that curve H is less linear than curve G especially at higher

electrical inputs. This may be the first indication of reduction such as is presumed to have happened to F.

The optimum procedure for polarizing PZT-4 seems to be a compromise between procedures G and H; i.e., a field strength of 40 KV/cm and a temperature not exceeding 110°C, with slow cooling to room temperature thereafter.

With further reference to Table IV, it may be seen that potential efficiency increases with increasing coupling coefficient, while total impedance at resonance and electrical Q decrease with increasing coupling coefficient. The mechanical Q and bandwidth of the transducer seem to have no particular relationship to coupling coefficient. It is believed that the high mechanical Q's measured are a function of transducer construction in that the PZT disc was cemented to a corprene backing which may be acting as a pressure release surface thereby not loading the disc completely. The data for potential efficiency, mechanical Q, electrical Q, bandwidth and impedance were obtained from the admittance vs frequency circles for radiation into water. These curves are presented as Figures 28 through 34.

Finally, it was noted that the frequency of radial resonance of the polarized discs varied with the square of the coupling coefficient. Figure 26 indicates the relationship between resonant frequency and k_r^2 is linear for coupling factors greater than 0.3. Figure 27 presents the same information somewhat differently. Using the frequency of radial resonance of disc "A" as reference, the percent change in resonant frequency is plotted versus k_r^2 and again it may be seen that the variation is linear.

8. Conclusions.

It has been found that the piezoelectric properties of the various lead zirconate titanate compositions are very stable over a wide range of temperatures. In addition PZT-4 and PZT-5 have piezoelectric properties much superior to those of barium titanate.

It has also been found that the loss factors of the lead zirconate titanate compositions are low and rise slowly with temperature. Although the electrical losses increase with voltage, as do the electrical losses of barium titanate, the loss factor of PZT-4 is extremely low even at high driving fields.

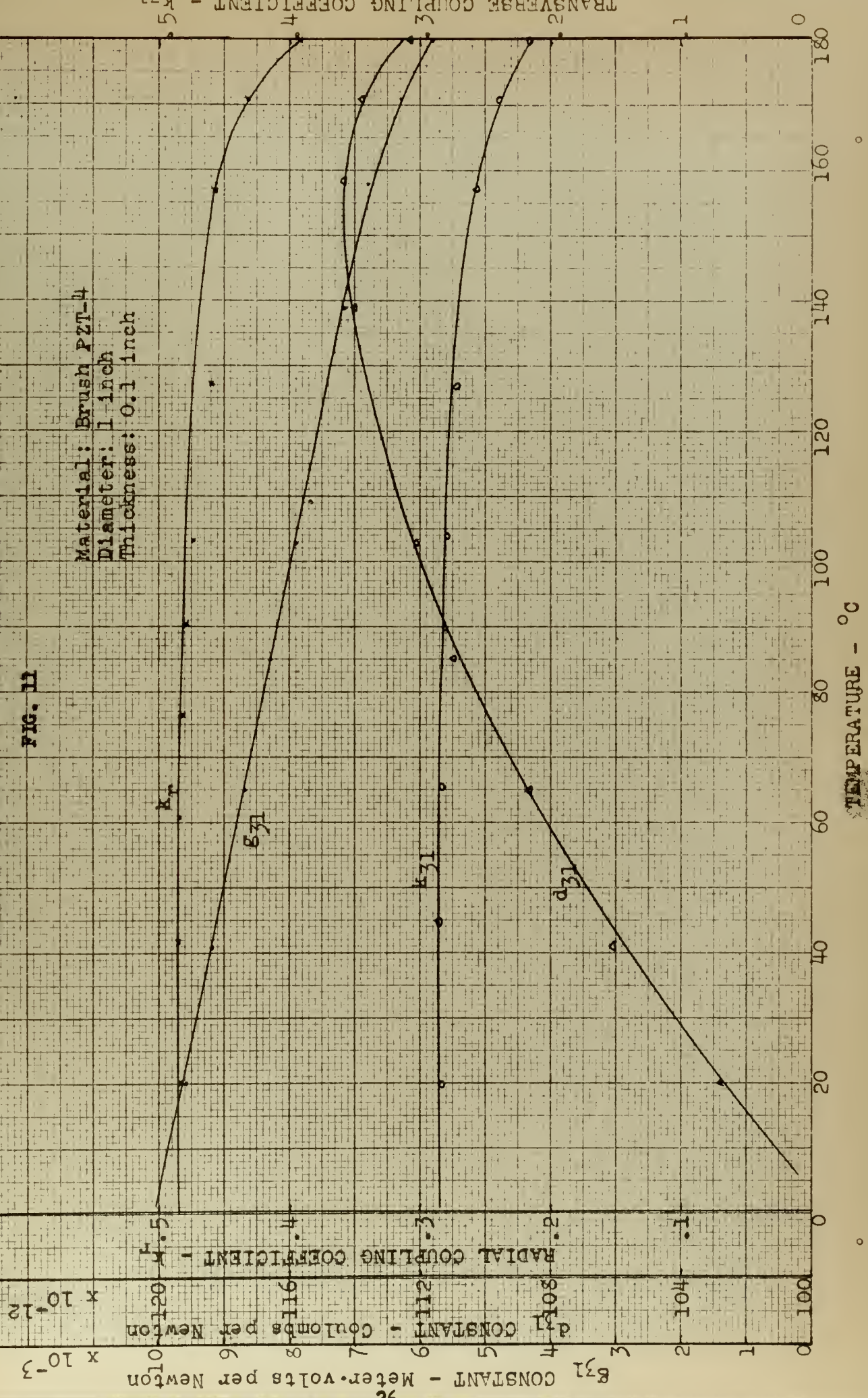
It has been found that PZT-4, in particular, has outstanding piezoelectric properties and is excellently suited for use in underwater acoustic transducers, sensing devices and hydrophones. In addition, because of its low loss factor and high temperature stability, it is one of the few materials suitable for high driving voltage and high power applications.

Finally, a very effective polarizing procedure for PZT-4 has been determined to be a field strength of 40 KV/cm applied throughout the temperature cycle, and a temperature not exceeding 110°C with slow cooling to room temperature thereafter.

RADIAL COUPLING COEFFICIENT, TRANSVERSE COUPLING COEFFICIENT, AND
 PIEZOELECTRIC COEFFICIENTS d_{31} & g_{31} vs. TEMPERATURE OF
 LEAD ZIRCONATE TITANATE COMPOSITION DISC

FIG. 11

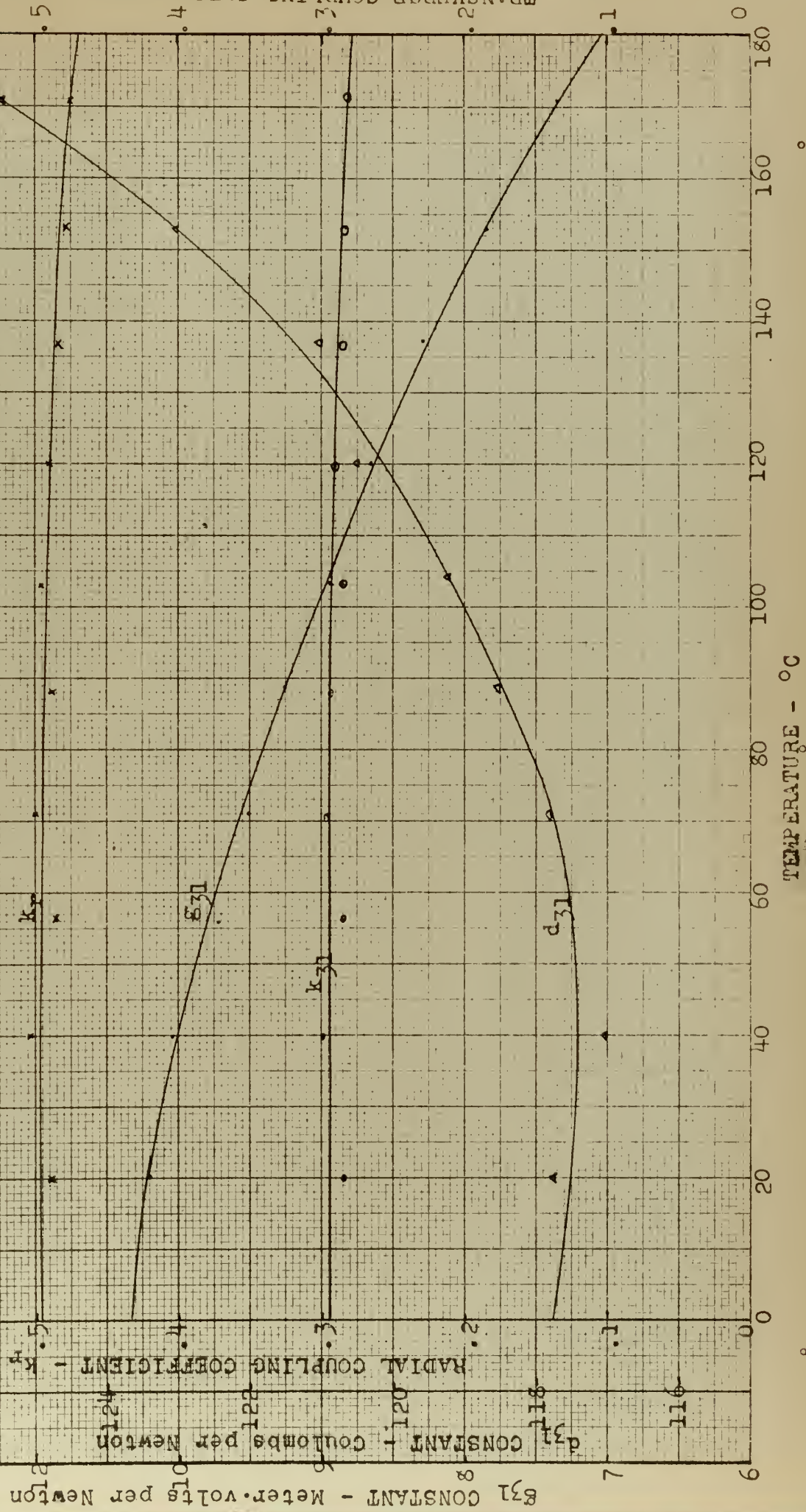
Material: Brush PZT-4
 Diameter: 1 inch
 Thickness: 0.1 inch



RADIAL COUPLING COEFFICIENT, TRANSVERSE COUPLING COEFFICIENT, AND
PIEZOELECTRIC COEFFICIENTS d_{31} & k_{31} vs. TEMPERATURE OF
LEAD ZIRCONATE TITANATE COMPOSITION DISC

FIG. 12

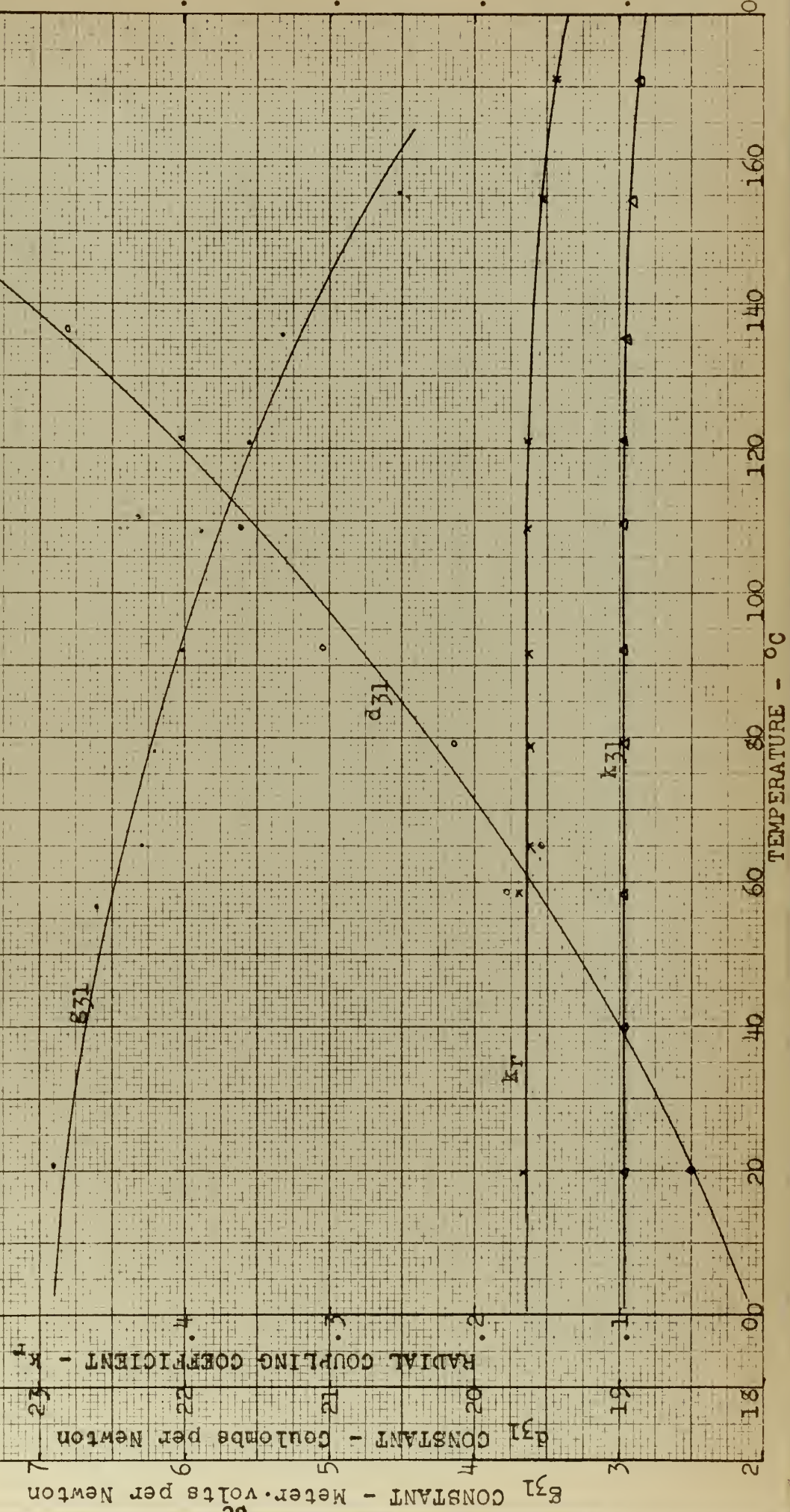
Material: Brush PZT-5A
Diameter: 1.77 inch
Thickness: 0.1 inch



RADIAL COUPLING COEFFICIENT, TRANSVERSE COUPLING COEFFICIENT, AND
PIEZOELECTRIC COEFFICIENTS d_{31} & g_{31} vs. TEMPERATURE OF
LEAD ZIRCONATE TITANATE COMPOSITION DISC

FIG. 13

Material: $Pb(Zr_{.55}Ti_{.45})O_3$
Diameter: 1.72 inch
Thickness: 0.12 inch

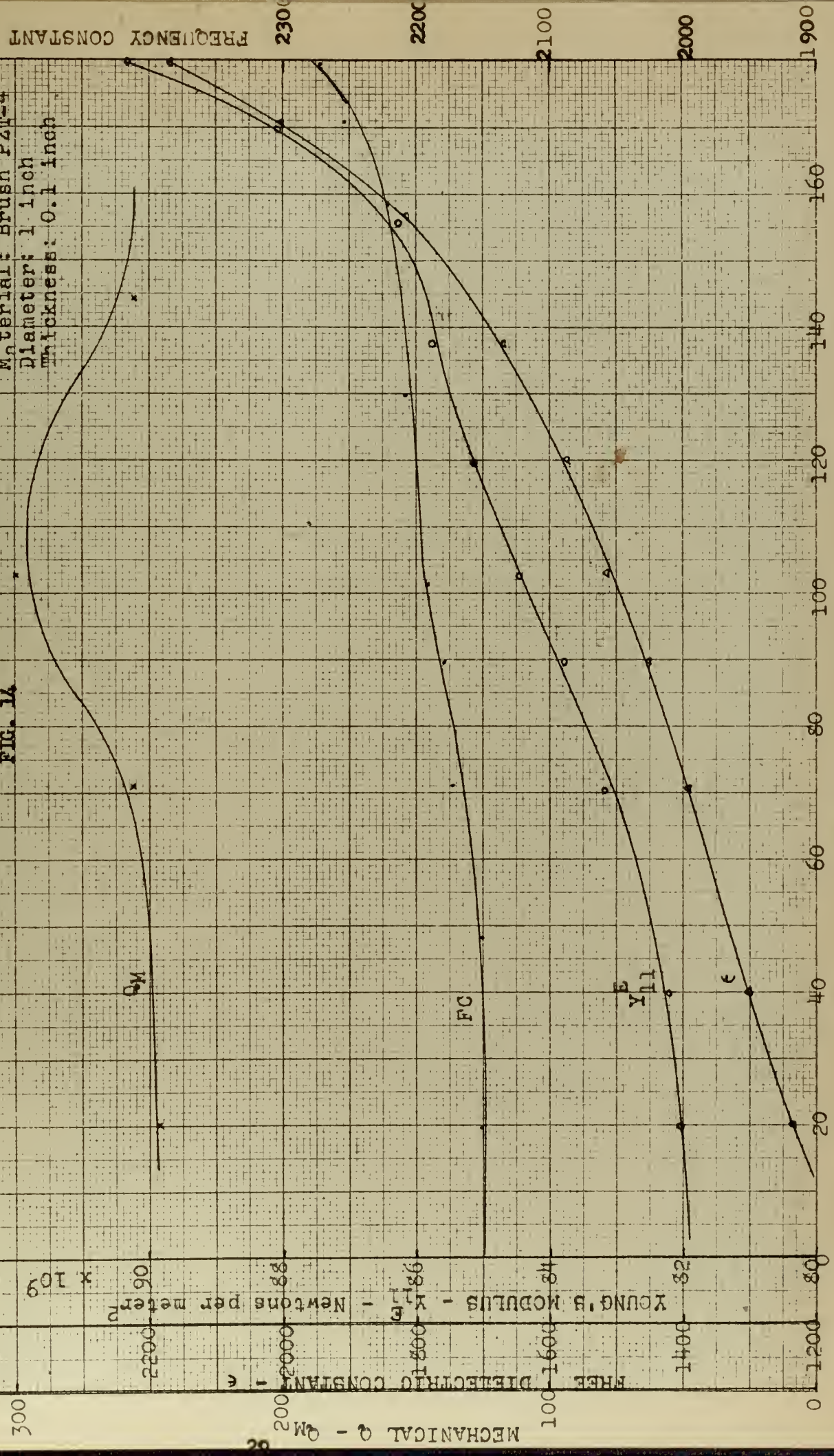




FREE DIELECTRIC CONSTANT, SHORT-CIRCUITED YOUNG'S MODULUS,
 FREQUENCY CONSTANT AND MECHANICAL Q vs. TEMPERATURE OF
 LEAD ZIRCONATE TITANATE COMPOSITION DISC

FIG. 1A

Material: Brush PZT-4
 Diameter: 1 inch
 Thickness: 0.1 inch

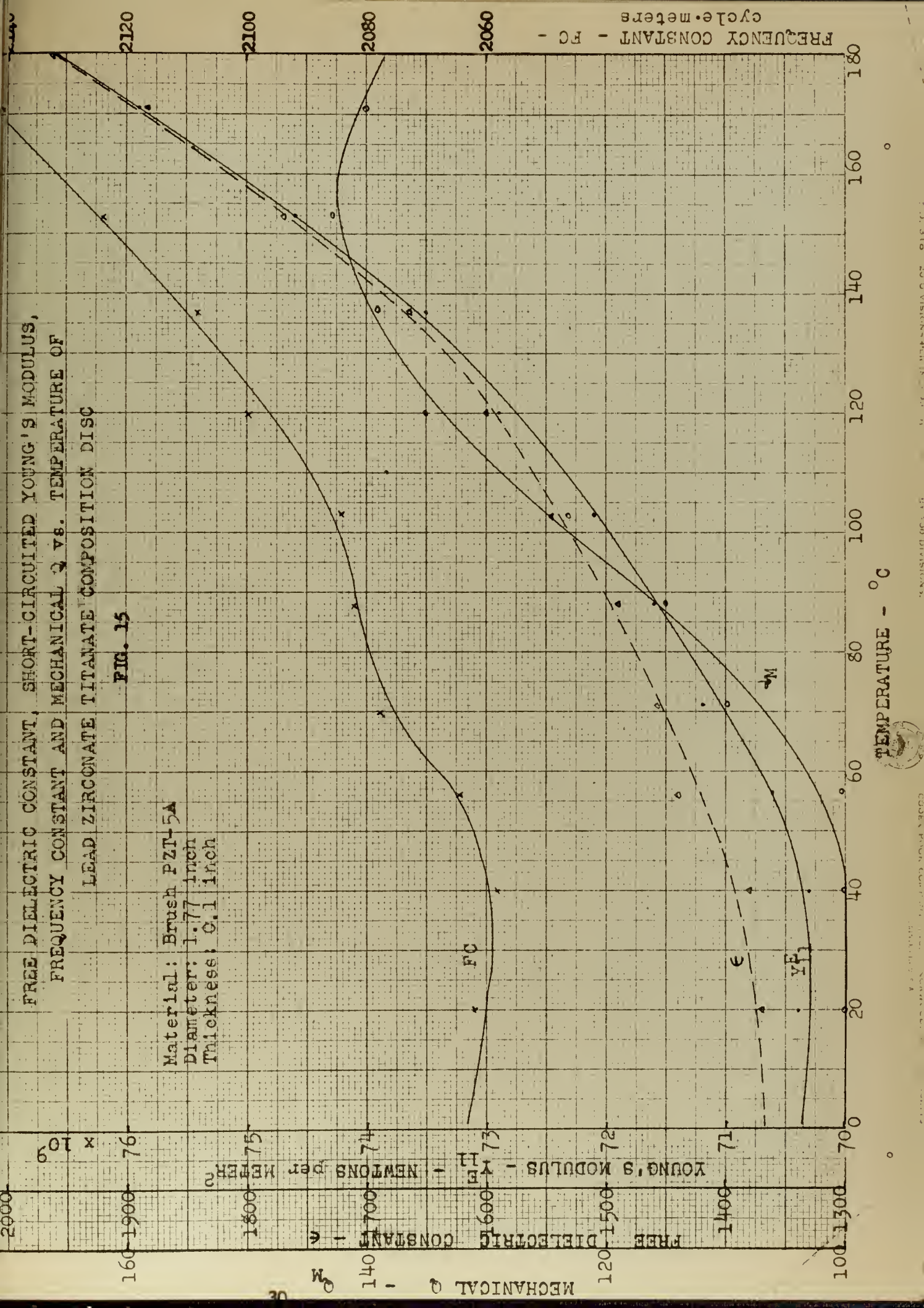


TEMPERATURE - °C

FREE DIELECTRIC CONSTANT, SHORT-CIRCUITED YOUNG'S MODULUS,
FREQUENCY CONSTANT AND MECHANICAL Q VS. TEMPERATURE OF
LEAD ZIRCONATE TITANATE COMPOSITION DISC

FIG. 15

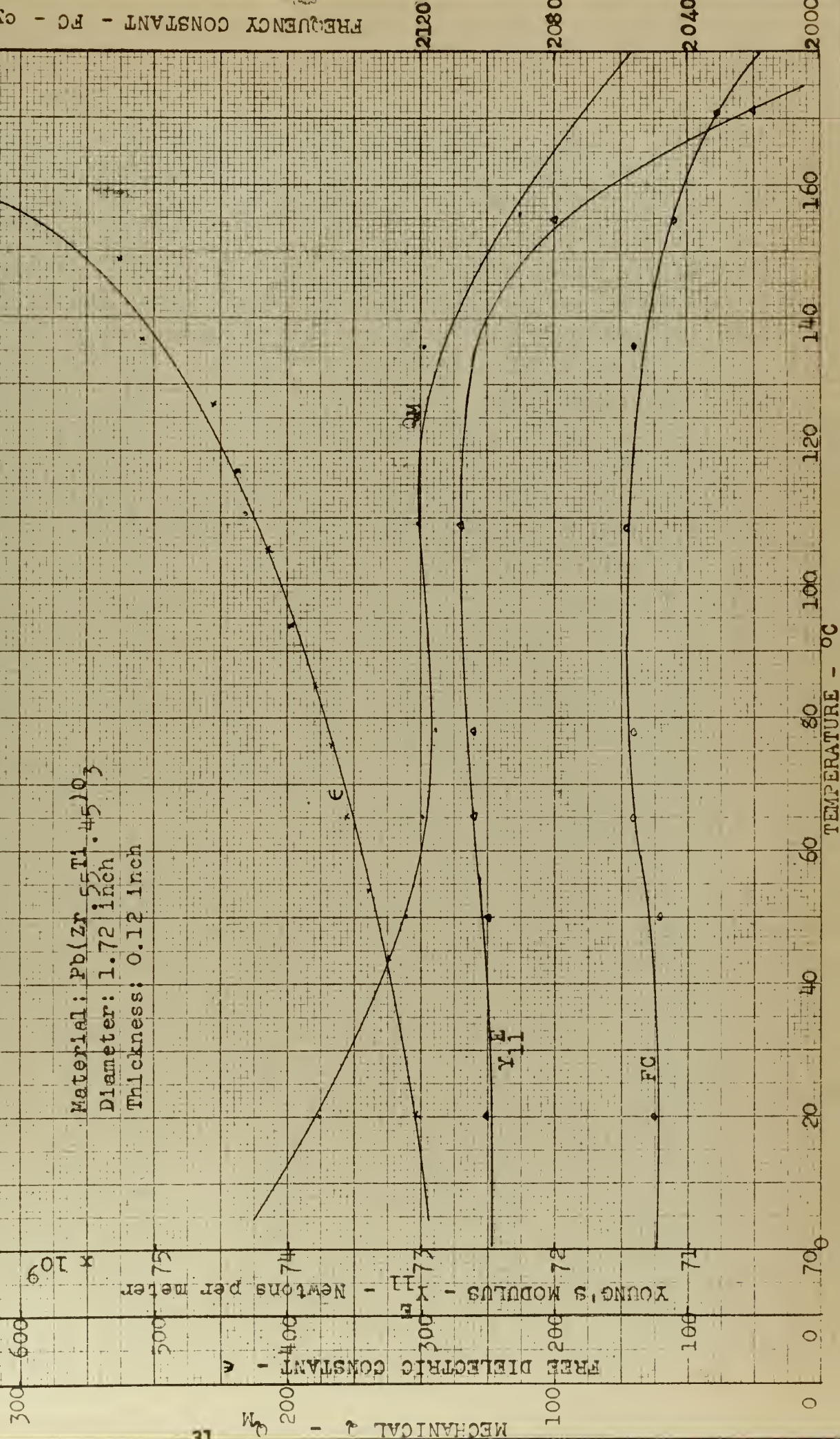
Material: Brush PZT-5A
Diameter: 1.77 inch
Thickness: 0.1 inch



FREE DIELECTRIC CONSTANT, SHORT-CIRCUITED YOUNG'S MODULUS,
FREQUENCY CONSTANT, AND MECHANICAL Q VS. TEMPERATURE OF
LEAD ZIRCONATE TITANATE COMPOSITION DISC

FIG. 16

Material: Pb(Zr₅₅Ti₄₅)₁₀₃
Diameter: 1.72 inch
Thickness: 0.12 inch



FREQUENCY CONSTANT - FC - cycle.meters

TABLE II

Comparison of Measured Piezoelectric and Dielectric Properties of Lead Zirconate
with Published Data of Barium Titanate 20°C

Coupling Coefficients		Strain Field	Force Field	Dielectric Constant	Tan δ at 1KC	Elastic Modulus $\frac{Y}{10^9}$ newton/meter ²	Mechanical Quality Q_m	Freq. Constant F·d	Curie Point $^{\circ}C$	Density 10^3 kg/m ³			
k_r	k_{31}	d_{31} 10 ⁻¹² coul/newt	g_{31} 10 ⁻³ volt·m/newton	ϵ				cps·m	$^{\circ}C$	10^3 kg/m ³			
<hr/>													
Pb(Zr _{.55} Ti _{.45})O ₃ (Laboratory Sample)													
	.165	.095	-	-18.5	-	6.85	305	.0045	72.5	280	2050	350	7.1
<hr/>													
PZT-4 (Brush Lab.)													
	.485	.285	.61	-102.7	-	9.7	1240	.002	82	250	2150	~300	7.64
<hr/>													
PZT-5A (Brush Lab.)													
	.495	.29	-	-117.5	-	10.4	1375	.01	70.6	100	2060	~300	7.6
<hr/>													
(Ba _{.92} Ca _{.08})TiO ₃ (Brush Ceramic B)													
	.33	.195	.45	-52.4	-	4.79	1235	<.01	116	1100	2300	118	5.5

TABLE III

Maximum Percentage Change* of Lead Zirconate Compositions in
the Temperature Range from 20°C to 120°C

	Coupling Coefficient Δk_T	Strain Field Δd_{31}	Force Field Δg_{31}	Dielec- tric Constant $\Delta \epsilon$	Loss Tangent $\Delta \tan \delta$	Elastic Modulus ΔY_0	Mechan- ical ΔQ_m	Frequency Constant ΔFC
	%	%	%	%	%	%	%	%
$Pb(Zr_{.55}Ti_{.45})O_3$	<.01	17.7	18.7	48	400	2.78	14.3	0.5
PZT-4	1.6	20.8	10	28.5	275	3.8	16	5.9
PZT-5A	1.0	15.3	2.3	16	110	3.0	34	1.7

*with respect to values listed in Table II

LOSS FACTOR vs. TEMPERATURE WITH A.C. FIELD AS A PARAMETER

FIG. 17

— Lead Zirconate Titanate,
Brush PZT-4

--- Barium Titanate, Brush Ceramic "B"
(Data taken from Baerwald &
Berlincourt JASA 25, 706-707
(1953))

LOSS FACTOR - TAN δ

TEMPERATURE - °C

1000 v/cm RMS

500 v/cm RMS

2000 v/cm RMS

500 v/cm RMS

100v/cm RMS

2000 v/cm RMS

1000 v/cm RMS

500 v/cm RMS

100 v/cm RMS

10 v/cm RMS

.07

.06

.05

.04

.03

.02

.01

0

200

180

160

140

120

100

80

60

40

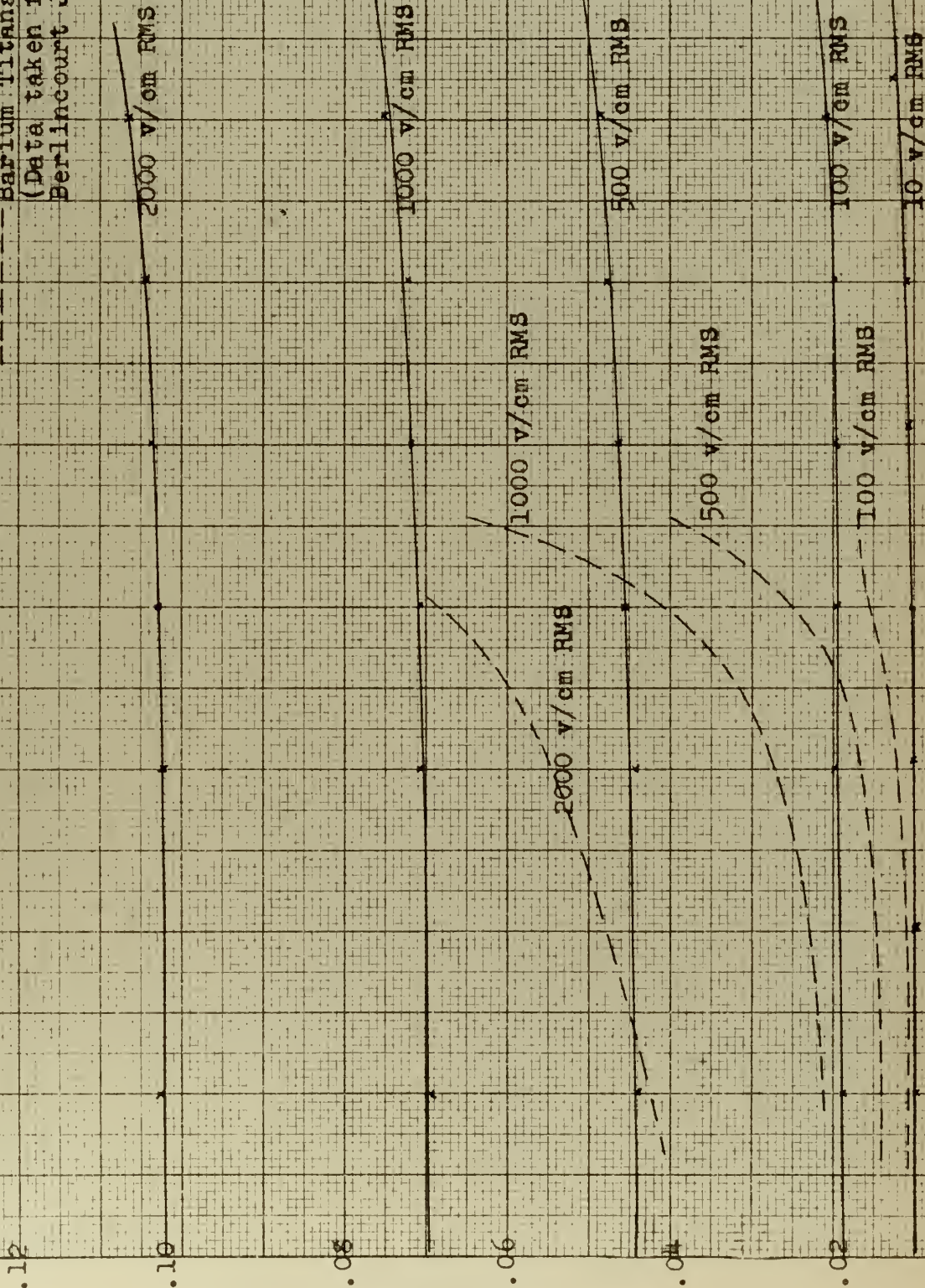
20

LOSS FACTOR vs. TEMPERATURE WITH A.C. FIELD AS A PARAMETER

FIG. 18

— Lead Zirconate Titanate,
Brush PZT-5A

--- Barium Titanate, Brush Ceramic "B"
(Data taken from Baerwald &
Berlincourt JASA 25, 706-707(1953))

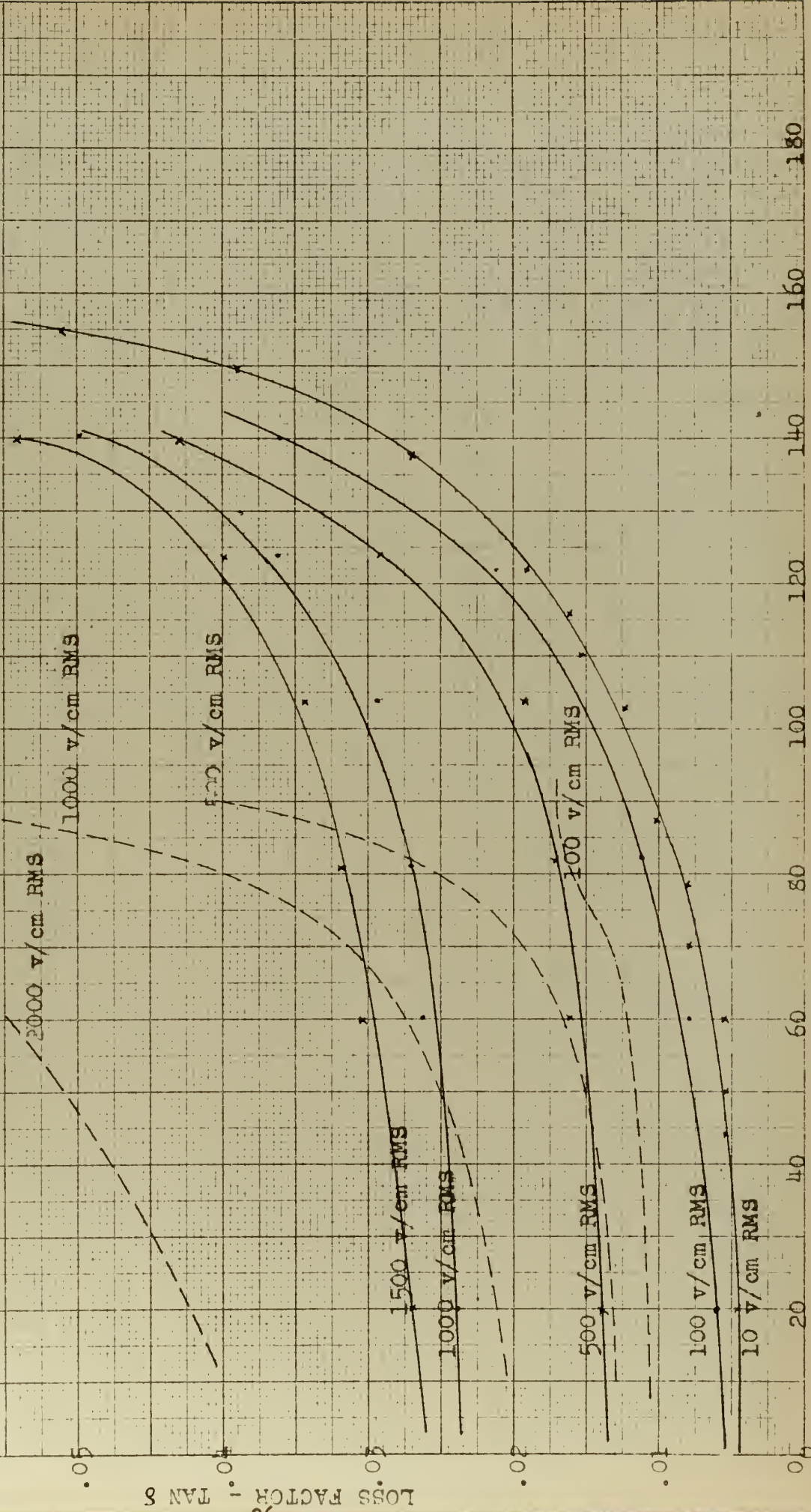


TEMPERATURE - °C

LOSS FACTOR vs. TEMPERATURE WITH A.C. FIELD AS A PARAMETER

FIG. 19

Lead Zirconate Titanate
Pb(Zr_{0.55}Ti_{0.45})O₃
Barium Titanate, Brush Ceramic "B"
(Data taken from Baerwald &
Berlincourt JASA 25, 706-707(1953))



TEMPERATURE - °C

LOSS FACTOR VS. A.C. FIELD WITH TEMPERATURE AS A PARAMETER

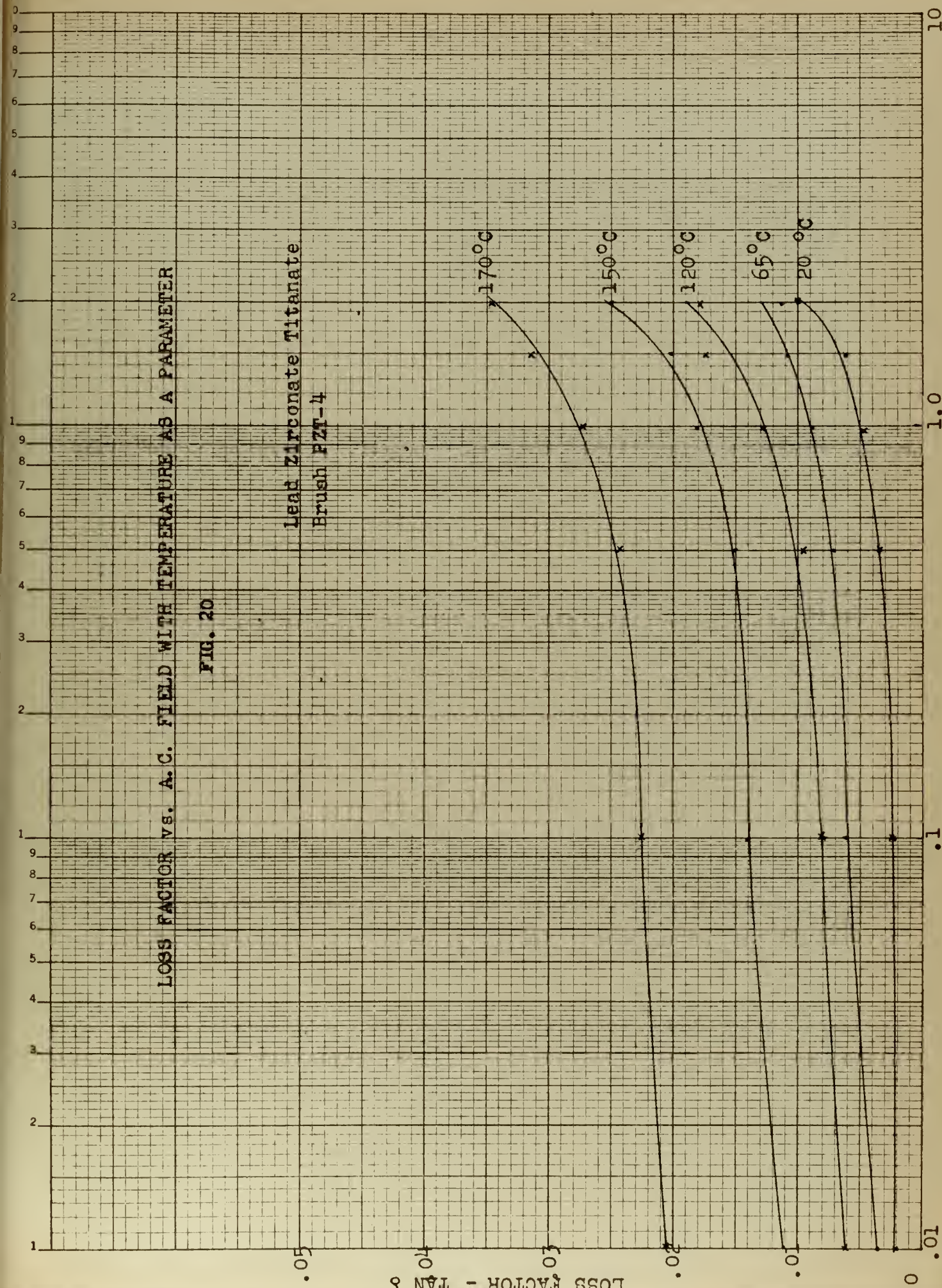
FIG. 20

Lead Zirconate Titanate
Brush PZT-4

LOSS FACTOR - TAN δ

RMS A.C. FIELD - Kv/cm

170°C
150°C
120°C
65°C
20°C



LOSS FACTOR VS. A.C. FIELD WITH TEMPERATURE AS A PARAMETER

FIG. 21

Lead Zirconate Titanate
Brush PZT-5A

150°C

20°C

LOSS FACTOR - TAN δ

RMS A.C. FIELD - Kv/cm

10

1.0

.1

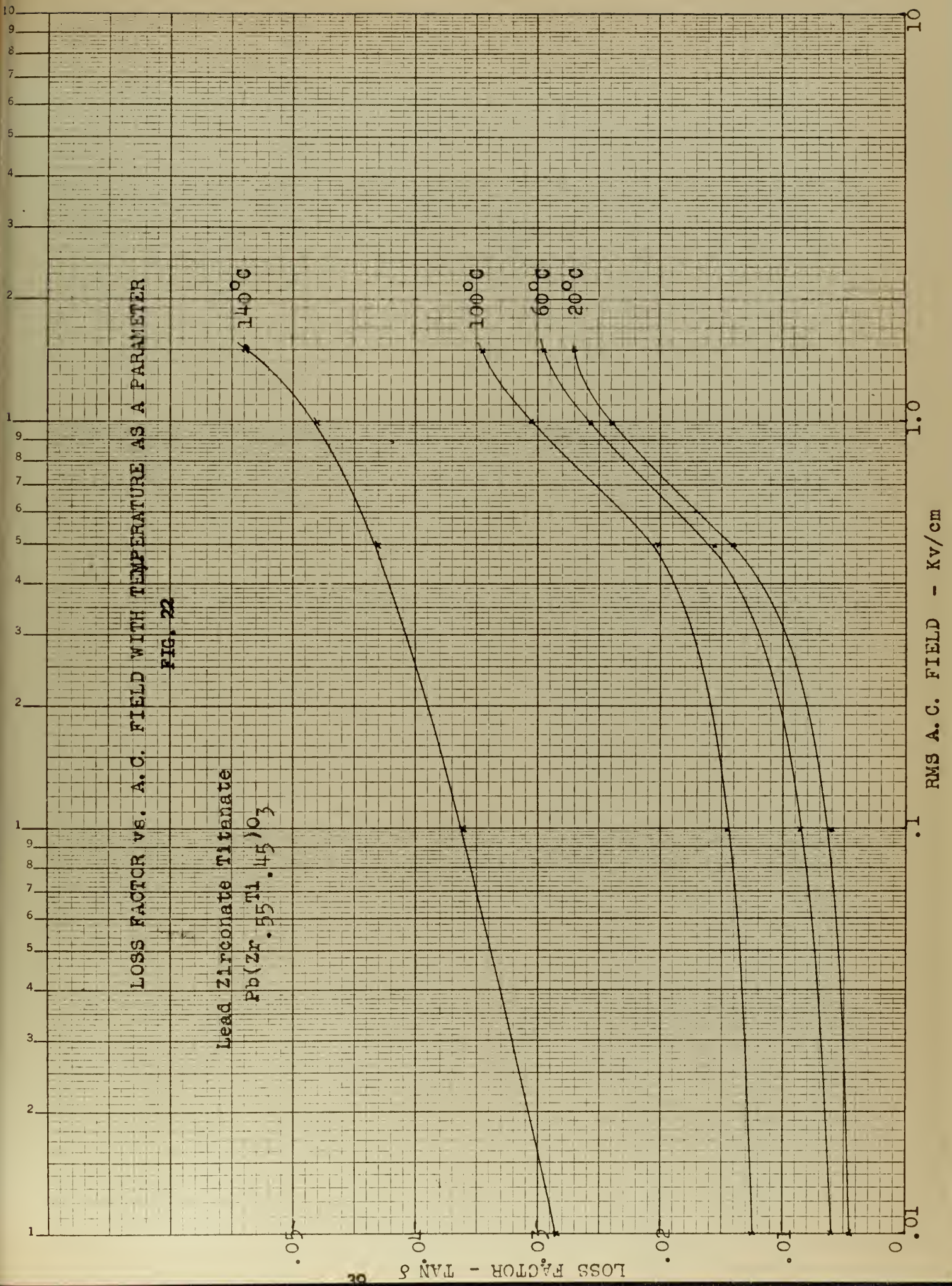
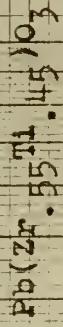
.01

1
2
3
4
5
6
7
8
9
1
2
3
4
5
6
7
8
9

LOSS FACTOR VS. A.C. FIELD WITH TEMPERATURE AS A PARAMETER

FIG. 22

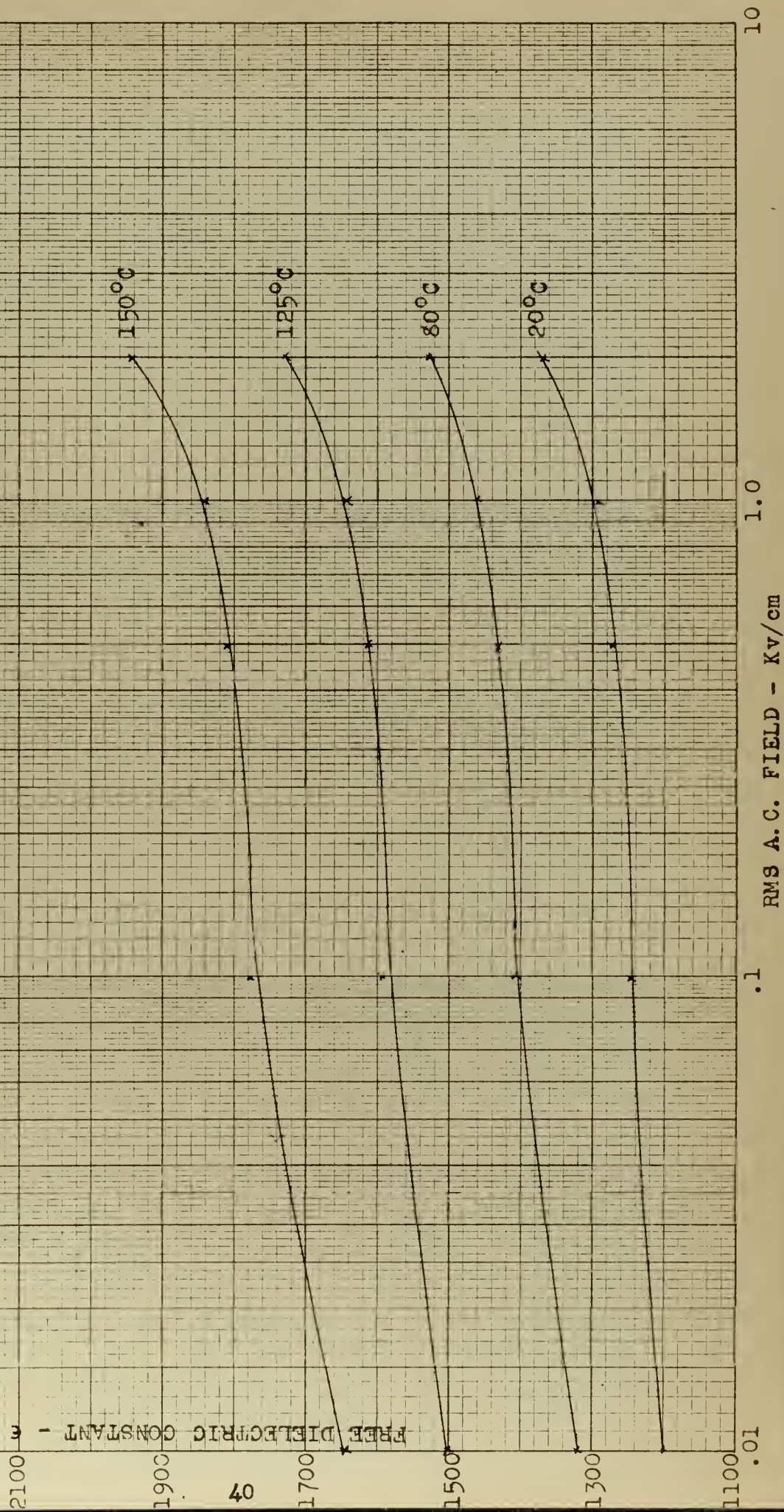
Lead Zirconate Titanate



FREE DIELECTRIC CONSTANT VS. A.C. FIELD WITH TEMPERATURE AS A PARAMETER

FIG. 23

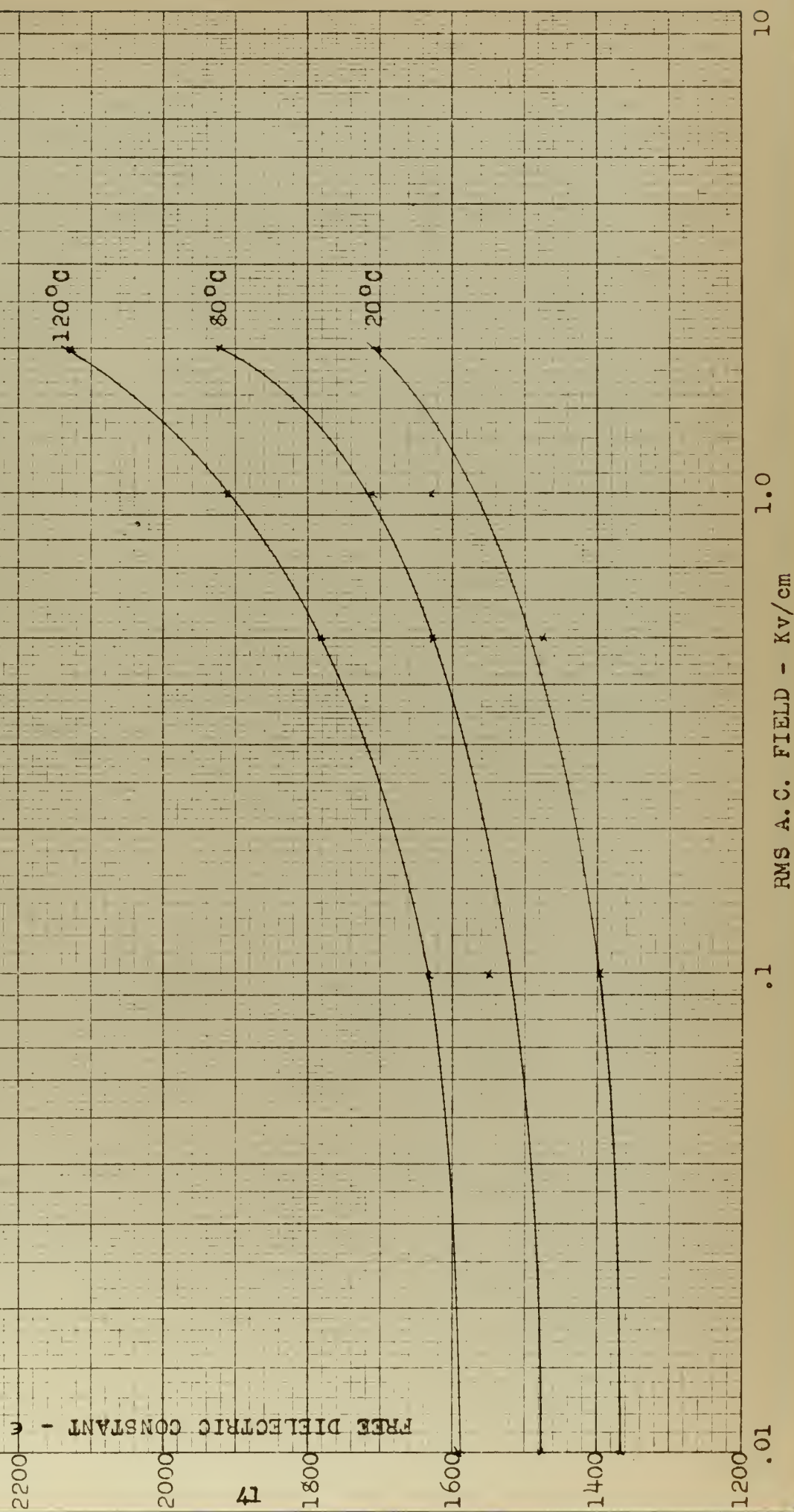
Lead Zirconate Titanate
Brush PZT-4



FREE DIELECTRIC CONSTANT VS. A.C. FIELD WITH TEMPERATURE AS A PARAMETER

FIG. 24

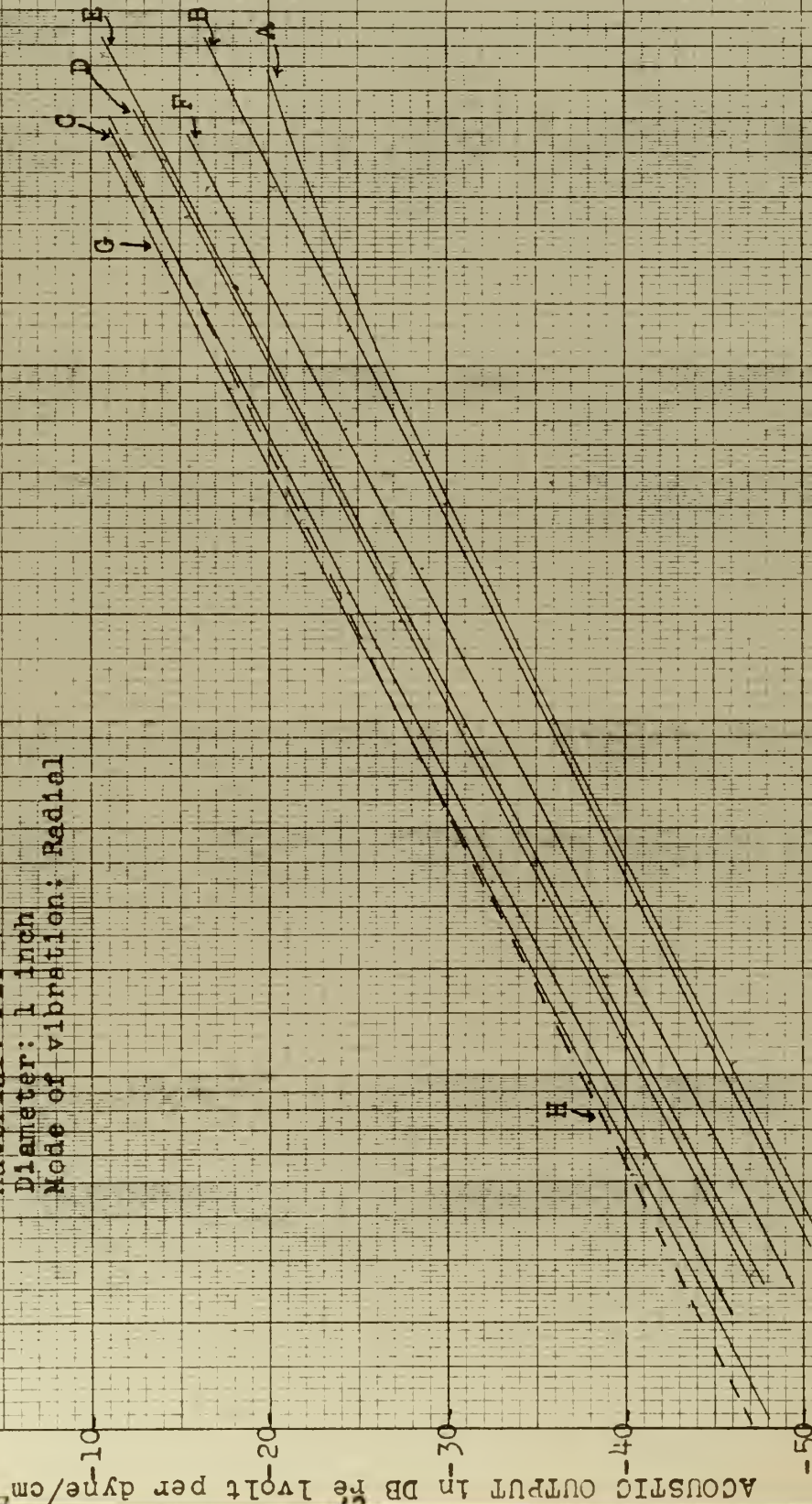
Lead Zirconate Titanate
Brush PZT-5A



ACOUSTIC OUTPUT VS. ELECTRICAL INPUT OF LEAD ZIRCONATE TITANATE DISCS WITH POLARIZATION PROCEDURE AS A PARAMETER

FIG. 25

Material: PZT-4
Diameter: 1 inch
Mode of vibration: Radial



ELECTRICAL INPUT - watts per centimeter²

0.001

0.01

0.1

1.0

10

ACOUSTIC OUTPUT in DB re 1 volt per dyne/cm²

TABLE IV

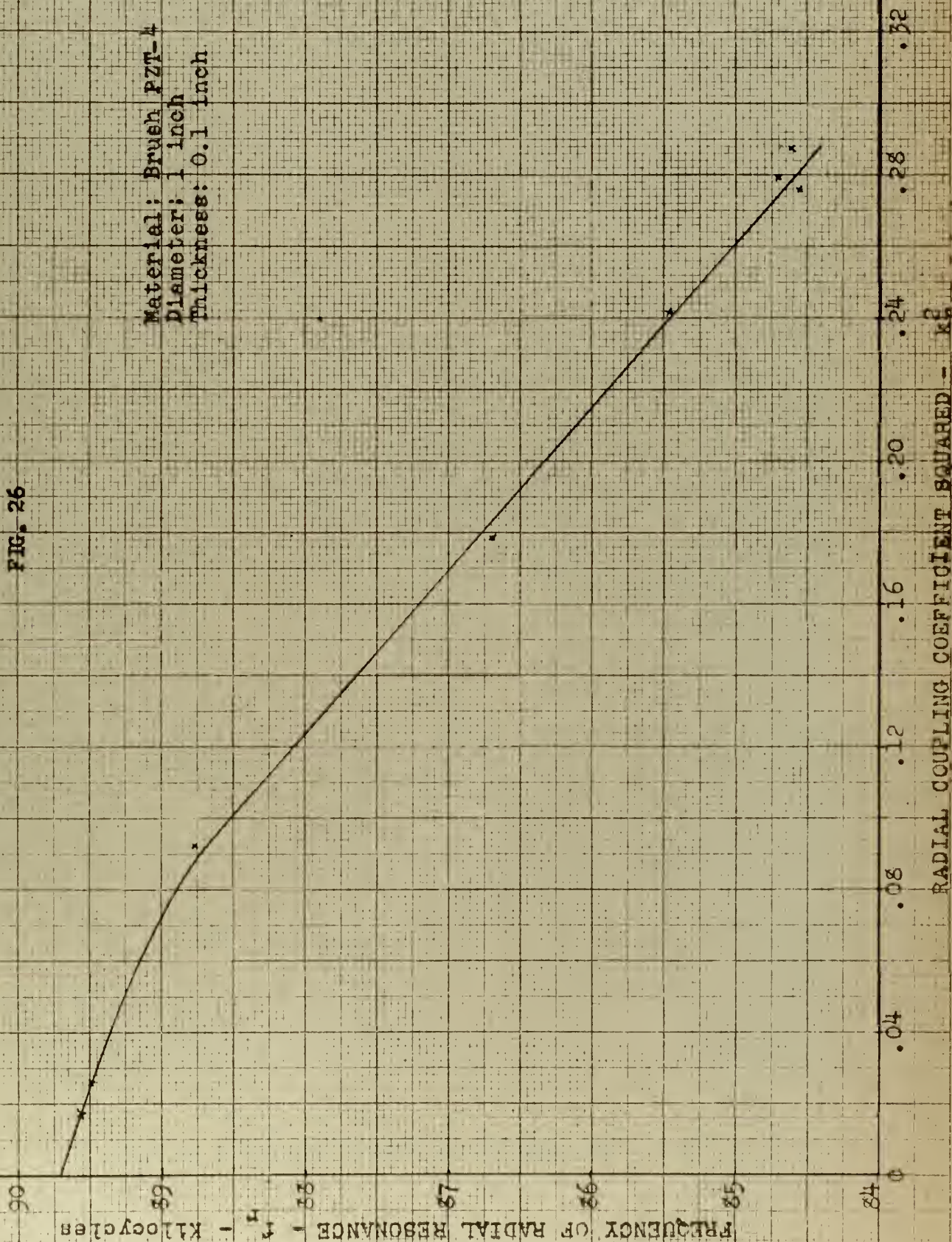
Results of Polarizing Procedures of PZT-4

Poling Procedure	Coupling Coefficient k_r	Potential Efficiency %	Mechanical Q	Electrical Q	Bandwidth Kcs	Total Impedance at Resonance Ohms
A	.129	-	-	-	-	-
B	.16	17.9	24.4	4.7	3.7	422 / 68.7°
F	.305	42	20.8	.985	4.3	368 / 44.6°
E	.423	72	23	.445	3.7	201 / 25°
D	.491	73	22.4	.316	3.85	196 / 19.5°
C	.525	74	21	.274	4.05	187 / 16.8°
G	.529	80.5	22.4	.254	3.45	136 / 12.4°
H	.538	80	23.6	.19	3.65	99 / 9.2°

FREQUENCY OF RADIAL RESONANCE VS. RADIAL COUPLING COEFFICIENT SQUARED OF LEAD ZIRCONATE TITANATE DISC

FIG. 26

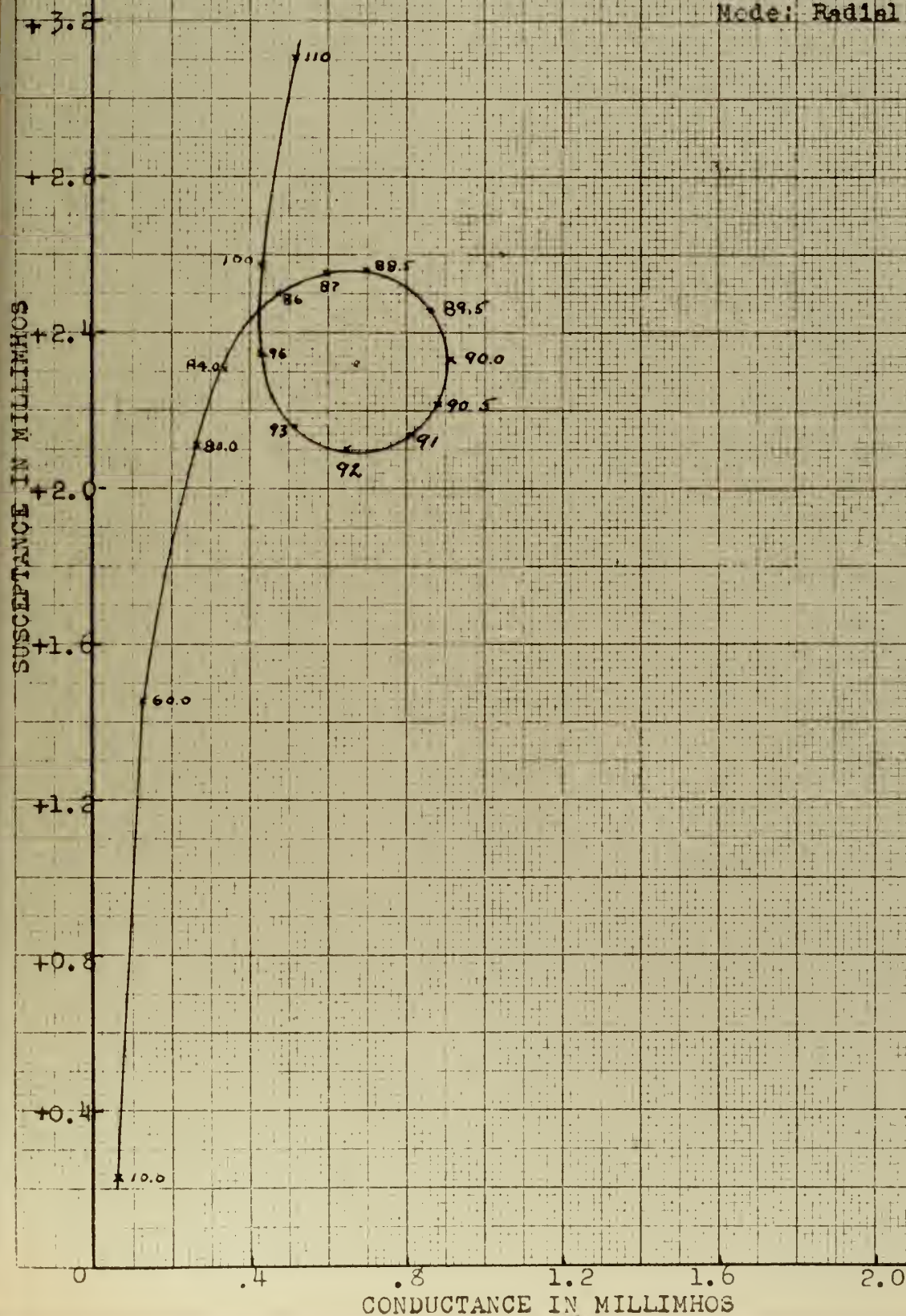
Material: Brush PZT-4
Diameter: 1 inch
Thickness: 0.1 inch



ADMITTANCE DIAGRAM IN WATER OF LEAD ZIRCONATE TITANATE
TRANSDUCER "B"

FIG. 28

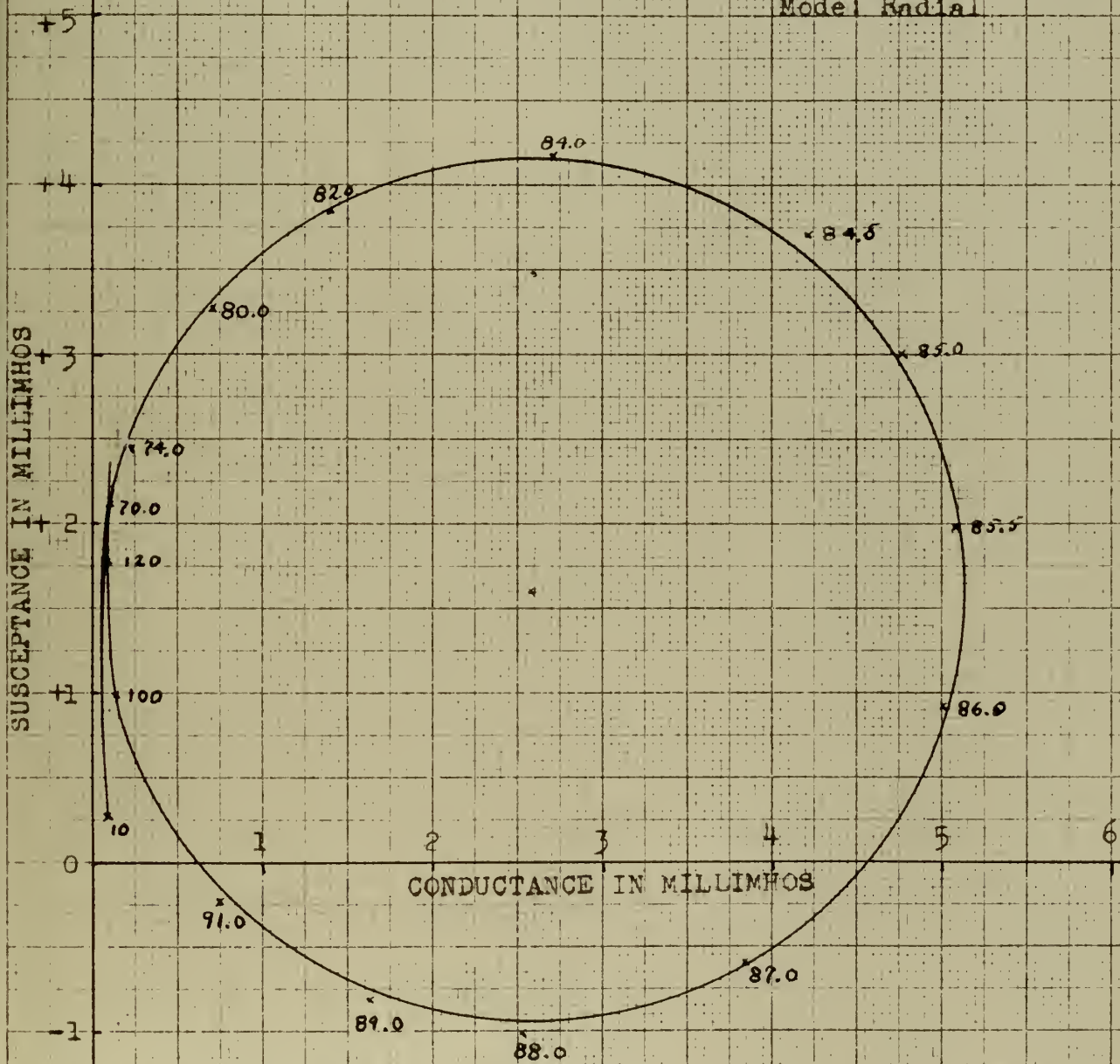
Material: Brush PZT-4
Diameter: 1 inch
Thickness: .096 inch
Mode: Radial



ADMITTANCE DIAGRAM IN WATER OF LEAD ZIRCONATE TITANATE
TRANSDUCER "C"

FIG. 29

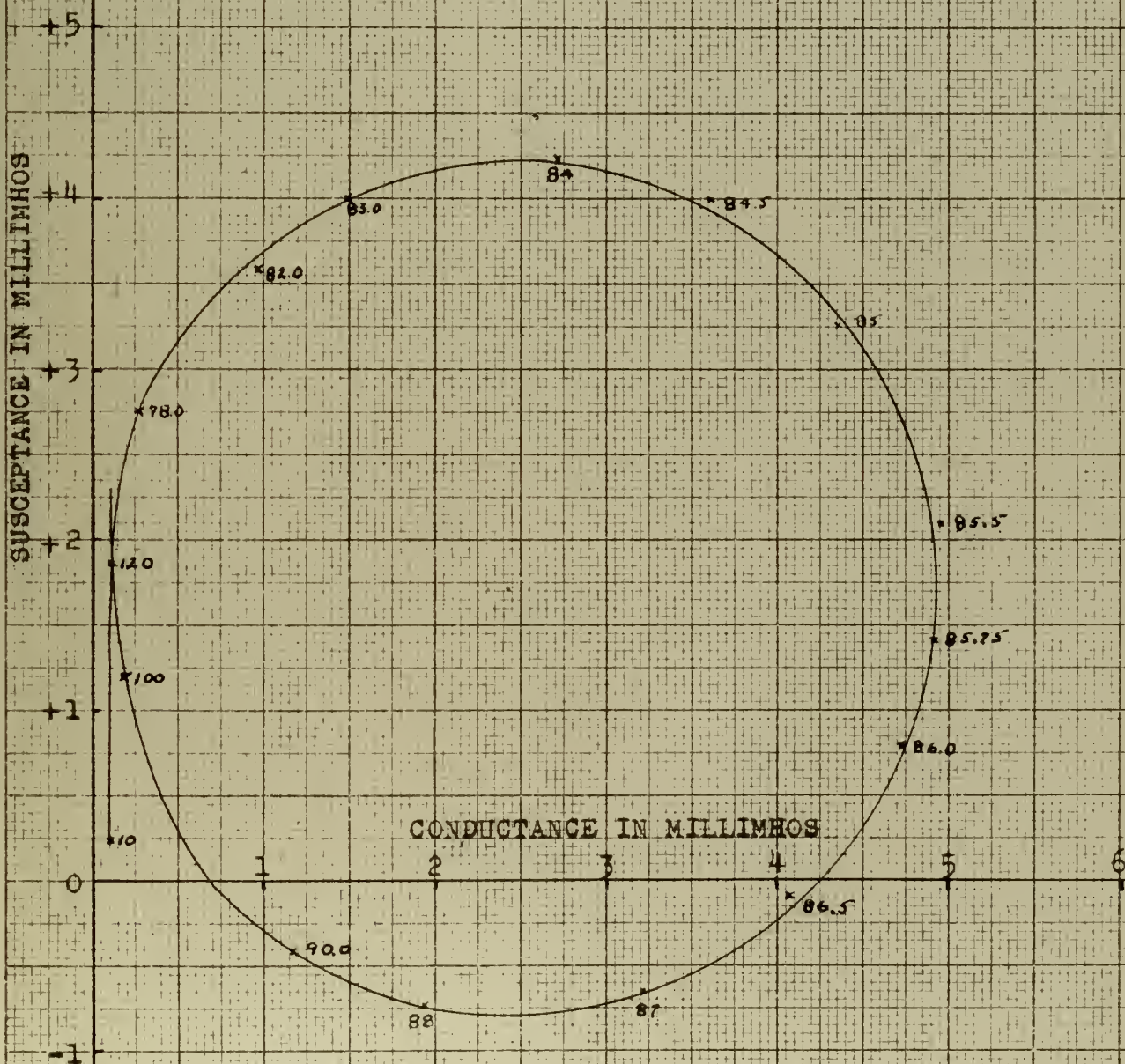
Material: Brush FZT-4
Diameter: 1 inch
Thickness: .096 inch
Mode: Radial



ADMITTANCE DIAGRAM IN WATER OF LEAD ZIRCONATE TITANATE TRANSDUCER "D"

FIG. 30

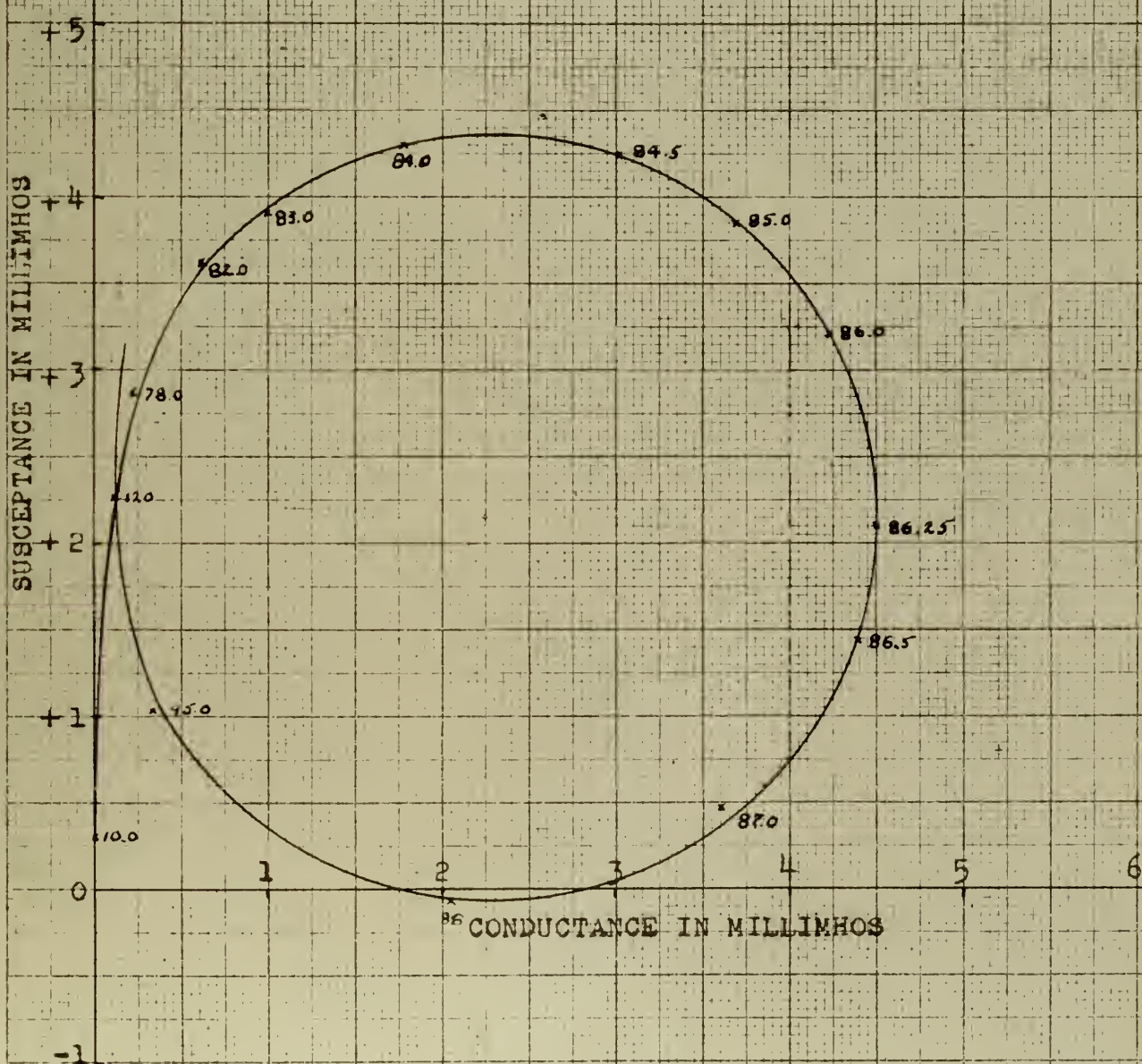
Material: Brush PZT-4
Diameter: 1 inch
Thickness: .096 inch
Mode: Radial



ADMITTANCE DIAGRAM IN WATER OF LEAD ZIRCONATE TITANATE TRANSDUCER "E"

FIG. 31

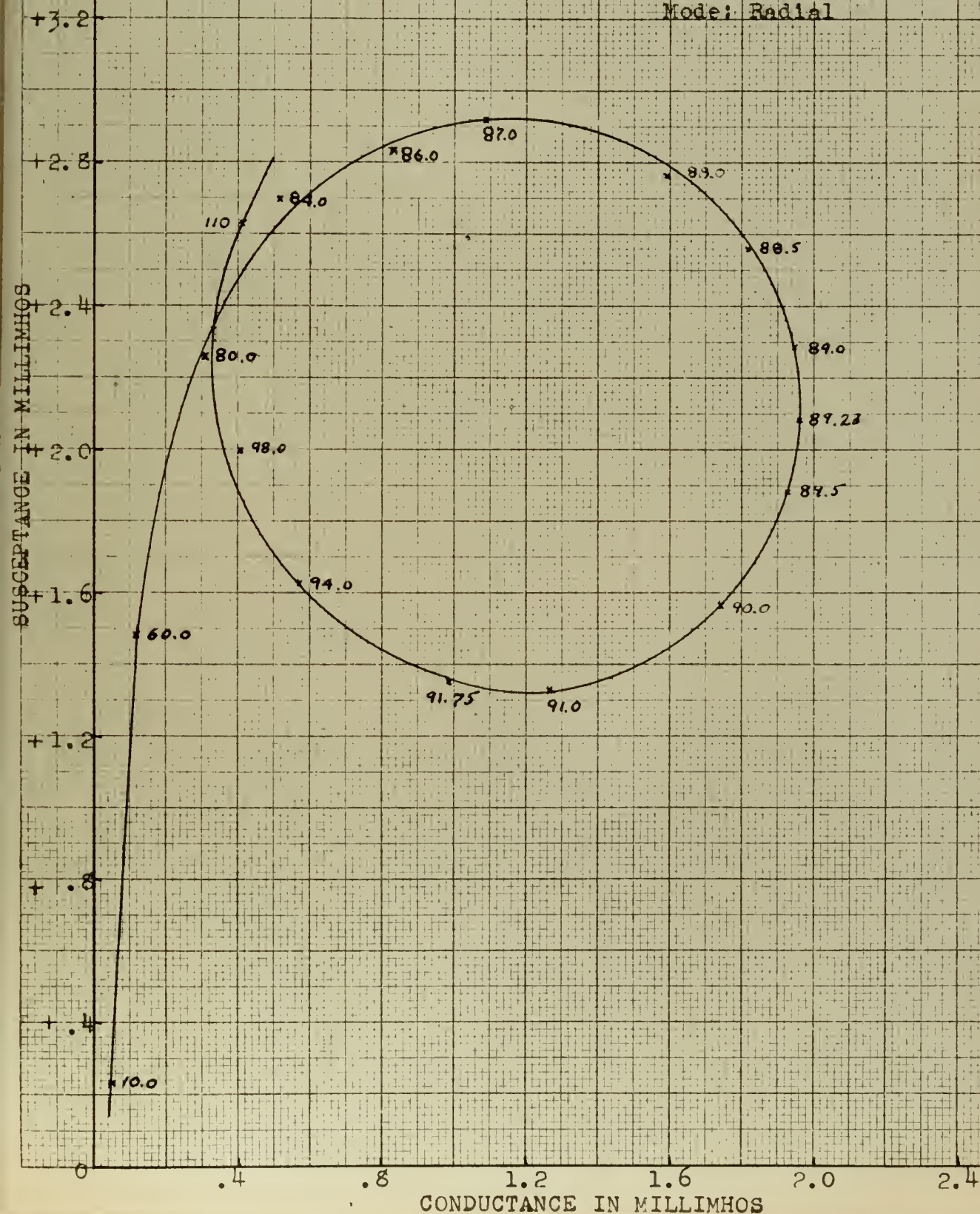
Material: Brush PZT-4
Diameter: 1 inch
Thickness: .071 inch
Mode: Radial



ADMITTANCE DIAGRAM IN WATER OF LEAD ZIRCONATE TITANTE
TRANSDUCER "F"

FIG. 32

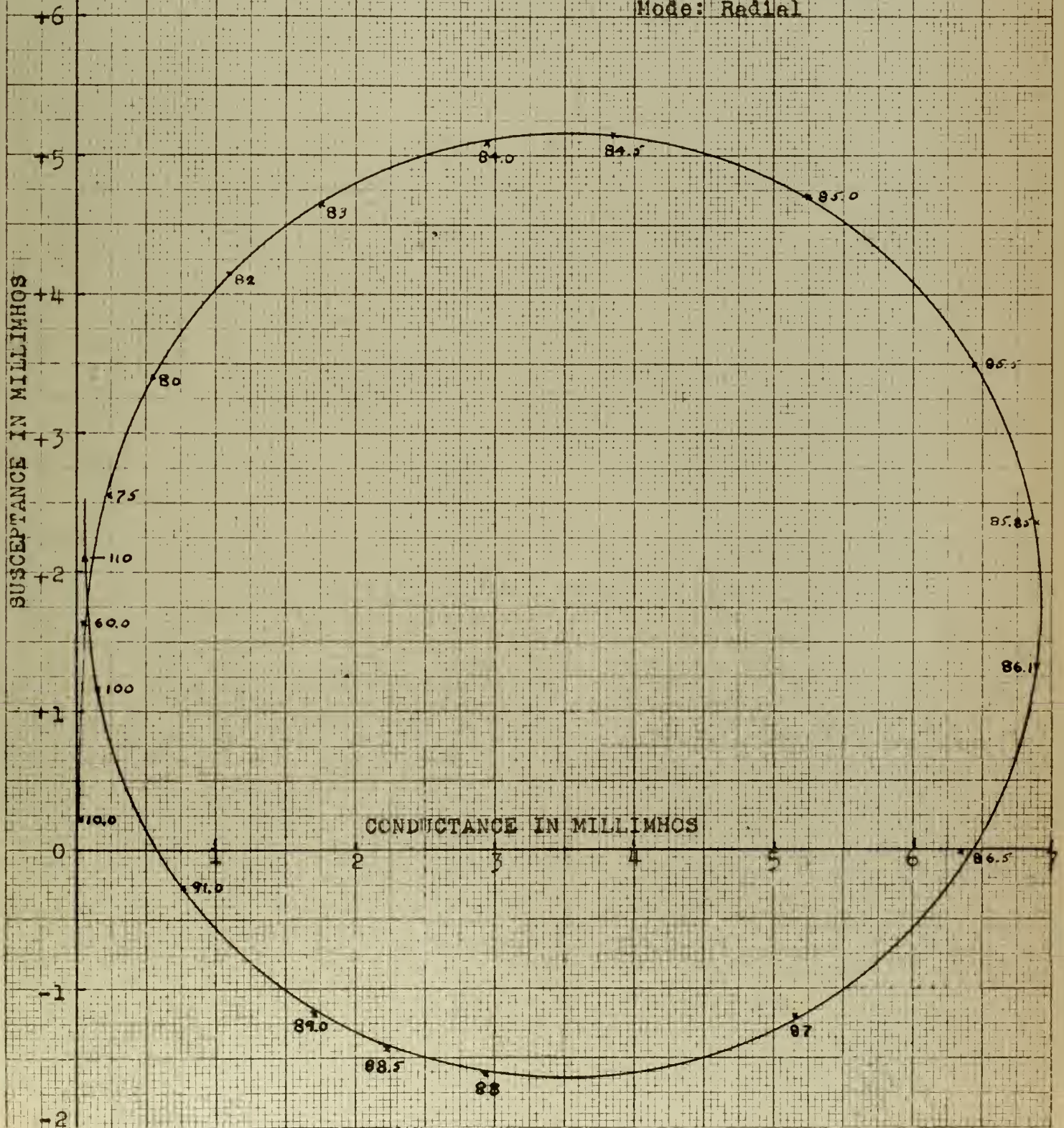
Material: Brush PZT-4
Diameter: 1 inch
Thickness: .096 inch
Mode: Radial



ADMITTANCE DIAGRAM IN WATER OF LEAD ZIRCONATE TITANATE TRANSDUCER "G"

FIG. 33

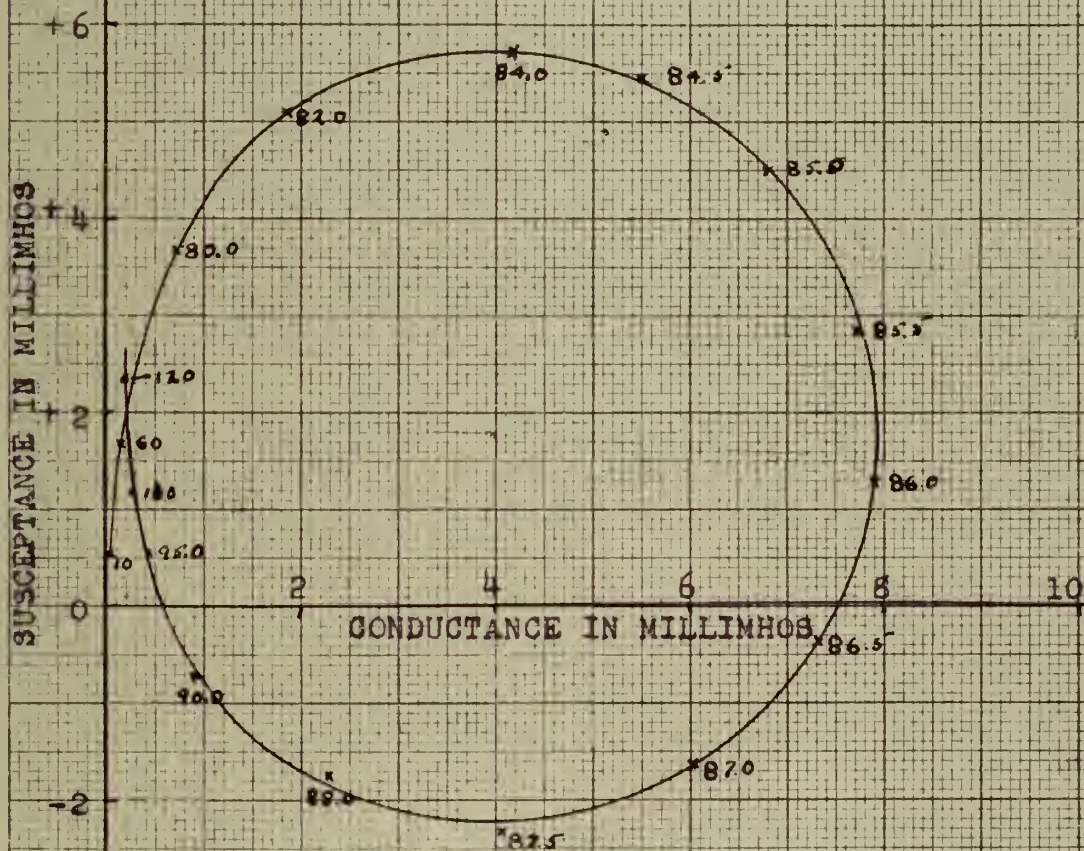
Material: Brush PZT-4
Diameter: 1 inch
Thickness: .1 inch
Mode: Radial



ADMITTANCE DIAGRAM IN WATER OF LEAD ZIRCONATE TITANATE TRANSDUCER "H"

FIG. 34

Material: Brush PZT-4
Diameter: 1 inch
Thickness: .1 inch
Mode: Radial



BIBLIOGRAPHY

1. H. G. Baerwald and D. A. Berlincourt, Electromechanical Response and Dielectric Loss of Prepolarized Barium Titanate Under Maintained Electric Bias, JASA [4] 25, pp. 703-710, July, 1953.
2. D. A. Berlincourt, Piezoelectric Titanate Ceramics with Low Temperature Coefficients, Brush Laboratories Company, Cleveland, Ohio, Technical Report No. 2, November 30, 1954.
3. D. A. Berlincourt, Recent Developments in Ferroelectric Transducer Materials, IRE Transactions on Ultrasonics Engineering, pp. 53-65, August, 1956.
4. R. J. Bobber, Dimensions of Test Tanks for Underwater Transducer Measurements, USRL Research Report #39 of 23 Aug 1956.
5. V. A. Bokov, Certain Piezoelectric Properties of Polycrystalline Solid Solutions of $(\text{Ba}, \text{Sr}) \text{TiO}_3$, $\text{Ba}(\text{Ti}, \text{Sn})\text{O}_3$ and $\text{Ba}(\text{Ti}, \text{Zr})\text{O}_3$, Soviet Physics - Acoustics, Vol. 3, No. 2, p. 112, April-June, 1957.
6. W. R. Buessem, et al, Study of the Degradation of High K Ceramic Dielectrics, Linden Laboratories, Inc., State College, Pa., Twelfth Quarterly Report of 15 Mar 1956.
7. Walter G. Cady, Piezoelectricity, McGraw-Hill Book Co., Inc., New York, 1946.
8. A. C. Dobelli, Piezoelectric Transducers, Acustica Vol. 6, No. 4, pp. 346-356, 1956.
9. J. G. Froemel, Polarization of Barium Titanate, Ultrasonic News, pp. 16-21, Nov., 1957.
10. A. L. Gray and J. M. Herbert, The Preparation of Barium Titanate as a Ceramic Transducer Material, Acustica Vol. 6, No. 2, pp. 229-276, 1956.
11. L. Hartshorn, Radio-Frequency Measurements by Bridge and Resonance Methods, John Wiley & Sons, Inc., New York, 1940.
12. J. W. Horton, Fundamentals of Sonar, United States Naval Institute, Annapolis, Md., 1957.
13. T. F. Hueter and R. H. Bolt, Sonics, John Wiley & Sons, Inc., New York, 1955.
14. T. F. Hueter, D. P. Neuhaus and J. Kolb, An Experimental Study of Polarization Effects in Barium Titanate Ceramics, JASA 26, 696, 1954.

15. F. V. Hunt, *Electroacoustics*, Harvard University Press, Cambridge, Mass., and John Wiley & Sons, Inc., New York, 1954.
16. IRE Standards on Piezoelectric Crystals: Determination of the Elastic, Piezoelectric, and Dielectric Constants - The Electro-mechanical Coupling Factor, 1958, *Proc IRE* 46, p. 764, 1958.
17. B. Jaffe, R. S. Roth and S. Marzullo, Piezoelectric Properties of Lead Zirconate - Lead Titanate Solid-Solution Ceramics, *J. Appl. Phys* [6] 25, pp. 809-810, 1954.
18. B. Jaffe, R. S. Roth and S. Marzullo, Improvement of Piezoelectric Ceramics, Report #8 for period Apr. 1 to June 30, 1954, National Bureau of Standards Report 3432, 1954.
19. B. Jaffe, R. S. Roth and S. Marzullo, Improvement of Piezoelectric Ceramics, Report #9 for period July 1 to Sept. 30, 1954, National Bureau of Standards Report 3684, 1954.
20. B. Jaffe, R. S. Roth and S. Marzullo, Properties of Piezoelectric Ceramics in the Solid-Solution Series Lead Titanate - Lead Zirconate - Lead Oxide: Tin Oxide and Lead Titanate - Lead Hafnate, *J. Research Nat. Bu. Standards*, 55, #5, pp. 239-249, Nov., 1955.
21. E. T. Jaynes, *Ferroelectricity*, Princeton University Press, Princeton, N. J., 1953.
22. L. E. Kinsler and A. R. Frey, *Fundamentals of Acoustics*, John Wiley & Sons, Inc, New York, 1950.
23. Charles Kittel, *Introduction to Solid State Physics*, Second Edition, John Wiley & Sons, Inc., New York, 1956.
24. Frank Kulcsar, Modified Piezoelectric Lead Titanate Zirconate Ceramics, Clevite Research Center, Cleveland, Ohio, Technical Report No. 14 of Dec. 2, 1957 for Office of Naval Research.
25. G. W. Marks, D. L. Waidelich and L. A. Manson, Investigations Concerning Polarization in Barium Titanate Ceramics, U.S. Navy Electronics Laboratory, San Diego, Report 729 of 26 Sept 1956.
26. Warren P. Mason, *Piezoelectric Crystals and Their Application to Ultrasonics*, D. Van Nostrand Co., Inc., New York, 1950.
27. W. P. Mason, Electrostrictive Effect in Barium Titanate Ceramics, *Phys. Rev.* [9] 74, pp. 1134-1147, Nov. 1948.
28. W. P. Mason and H. Jaffe, Methods for Measuring Piezoelectric Elastic, and Dielectric Coefficients of Crystals and Ceramics, *Proc. IRE* 42, pp. 921-930, 1954.
29. OSRD - Summary Technical Report of Division 6, NDRC, Vol. 13, The Design and Construction of Magnetostriction Transducers, Washington, D. C., 1946. RESTRICTED

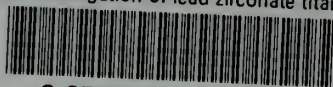
30. C. F. Pulvari, Ferroelectric Materials Survey with Particular Interest in their Possible Use at High Temperatures, WADC Technical Note 56-467 (ASTIA Document #110489) of Feb., 1957.
31. G. W. Renner, R. A. Plante, and T. F. Hueter, The Power Handling Capability of Ferroelectric Ceramics, IRE National Convention Record 1958, (to be published).
32. S. Roberts, Dielectric Properties of Lead Zirconate and Barium Lead Zirconate, J. Am. Ceram. Soc. [2], 33, p. 63, 1950.
33. N. A. Roi, Dielectric and Piezoelectric Properties of Solid Solutions of $(\text{Ba}, \text{Sr})\text{TiO}_3$, $(\text{Ba}, \text{Pb})\text{TiO}_3$, $\text{Ba}(\text{Ti}, \text{Sn})\text{O}_3$ and $\text{Ba}(\text{Ti}, \text{Zn})\text{O}_3$, Soviet Physics - Acoustics, Vol. 2, No. 1, 60, 1956.
34. E. Sawaguchi, Ferroelectricity vs Antiferroelectricity in the Solid Solution of PbZrO_3 and PbTiO_3 , J. Phys. Soc., Japan 8, pp. 615-629 Sept.-Oct., 1953.
35. E. Sawaguchi, H. Maniwa and S. Hoshine, Antiferroelectric Structure of Lead Zirconate, Phys. Rev. [5], 83, p. 1078, 1951.
36. D. Schofield, R. F. Brown, and W. H. Dingle, An Investigation of Some Barium Titanate Compositions for Underwater Transducer Applications, Part I of March, 1956, Naval Research Establishment, Dartmouth, N. H., Report TM56/3 (RESTRICTED)
37. D. Schofield, R. F. Brown, and W. H. Dingle, An Investigation of Some Barium Titanate Compositions for Underwater Transducer Applications, Part II of June, 1956, Naval Research Establishment, Dartmouth, N. H., Report TM56/7 (RESTRICTED)
38. G. Shirane, Dielectric Properties of Lead Zirconate, Phys. Rev., 86, p. 219, 1952.
39. G. Shirane, F. Jona, and R. Pepinsky, Some Aspects of Ferroelectricity, Proc. IRE 43, pp. 1738-1793, Dec., 1955.
40. G. Shirane, E. Sawaguchi and Y. Takago, Dielectric Properties of Lead Zirconate, Phys. Rev., 84, p. 476, 1951.
41. G. Shirane, & K. Suzuke, Crystal Structure of $\text{Pb}(\text{Zr}, \text{Ti})\text{O}_3$, J. Phys. Soc., Japan, 7, pp. 336-337, 1952.
42. G. Shirane, K. Suzuke and A. Takeda, Phase Transitions in Solid Solutions of PbZrO_3 and PbTiO_3 , II X-Ray Study, J. Phys. Soc. Japan, 7, pp. 12-18, Jan.-Feb., 1952)
43. G. Shirane and A. Takeda, Phase Transitions in Solid Solutions of PbZrO_3 and PbTiO_3 , I. Small Concentration of PbTiO_3 , J. Phys. Soc. Japan, 7, pp. 5-11, Jan.-Feb., 1952.

44. A. Vernon, Ferroelectricity, Amer.Jour. Phys., 23, p. 183, April 1953.
45. A. VonHippel, Dielectric Materials and Their Applications, Technology Press of MIT and John Wiley & Sons, Inc., New York.



thesR2455

An investigation of lead zirconate titan



3 2768 002 05320 9

DUDLEY KNOX LIBRARY